Supplementary Information (SI) for Organic Chemistry Frontiers.

Iminophosphorane in Perylenediimide Chemistry: Staudinger Reaction and a Visible-Light-Driven Competitive Reaction of the Cadogan Cyclization

Maxime Roger,[1] Oksana Krupka,[2] Olivier Alévêque,[1] Eric Levillain,[1] and Piétrick Hudhomme[1,*]

[1] *Univ Angers, CNRS, MOLTECH-Anjou, SFR MATRIX, F-49000 Angers, France.*
E-mail: pietrick.hudhomme@univ-angers.fr
[2] *Univ Angers, Inserm, CNRS, MINT, SFR ICAT, F-49000 Angers, France.*

Experimental details

Table of content

I. Materials and Methods

Chemicals were purchased from Avocado (sodium azide), Alfa Aesar (triphenylphosphine).

NitroPDI **1** was prepared according to literature.[1]

Solvents were purchased from Fisher Scientific (DMF HPLC grade, MeOH HPLC grade, THF HPLC grade, CH_2Cl_2 HPLC grade), Carlo Erba ($CHCl_3$, CH_2Cl_2), deuterated solvent ($CDCl_3$) from Sigma Aldrich. THF was dried over Na/benzophenone.

Thin layer chromatography (TLC) was conducted on pre-coated aluminum sheets with 0.20 mm Merck Alugram SIL G/UV254 with fluorescent indicator UV254. Column chromatography was carried out using Sigma-Aldrich silica gel 60 (particle size 63-200 μm).

Nuclear magnetic resonance (NMR) ^{1}H, ^{13}C, ^{31}P spectra were obtained on a Bruker 300 MHz Avance III spectrometer (300 MHz for ^{1}H and 75 MHz for ^{13}C) or 500 MHz Advance III HD spectrometer (500 MHz for ^{1}H, 125 MHz for ^{13}C, 202.4 MHz for ^{31}P). ^{13}C and ^{31}P spectra were recorded with a complete decoupling for the proton. ^{19}F spectra were recorded on a Bruker 300 MHz Avance III spectrometer (283 MHz for ^{19}F). Chemical shifts were reported in ppm according to tetramethylsilane using the solvent residual signal as an internal reference ($CDCl_3$: ^{1}H = 7.26 ppm, ^{13}C = 77.16 ppm). Coupling constants (J) were given in Hz. Resonance multiplicity was described as s (singlet), d (doublet), t (triplet), q (quartet), tt (triplet of triplet), m (multiplet) and br.s. (broad singlet).

MALDI-TOF spectra were performed on a Bruker Daltonics Biflex III (SFR Matrix, MOLTECH-Anjou, Angers) using DCTB (trans-2-[3-(4-tert-butylphenyl)-2-methyl-2-propenylidene]malononitrile) as matrix. High resolution mass spectrometry (HRMS) was performed with a JEOL JMS-700 B/E.

UV-Visible absorption spectra were recorded on a Shimadzu UV-1800 UV-Vis spectrophotometer using quartz cell (pathlength of 1 cm).

Fluorescence was measured on a Shimadzu RF-6000 Spectrophotometer using quartz cell (pathlength of 1 cm).

Cyclic voltammetry experiments were carried out at room temperature in a glove box on a Bio-Logic SAS SP-150 potentiostat, with Pt electrode and counter-electrode and Ag as a reference electrode using 0.1 M *n*-Bu_4NPF_6 in CH_2Cl_2 as supporting electrolyte.

Thermogravimetric analyses (TGA) were carried out with a TA instruments Q500 apparatus under nitrogen atmosphere at a heating rate of 10 ºC/min from room temperature up to 1000ºC.

[1] El-Berjawi, R.; Hudhomme, P., *Dyes and Pigments* **2018,** *159*, 551-556.

The irradiation was done with a HCK1012-01-005 EvoluChem LED Spotlight (18 W) from HepatoChem
Its absorption spectrum is given below :

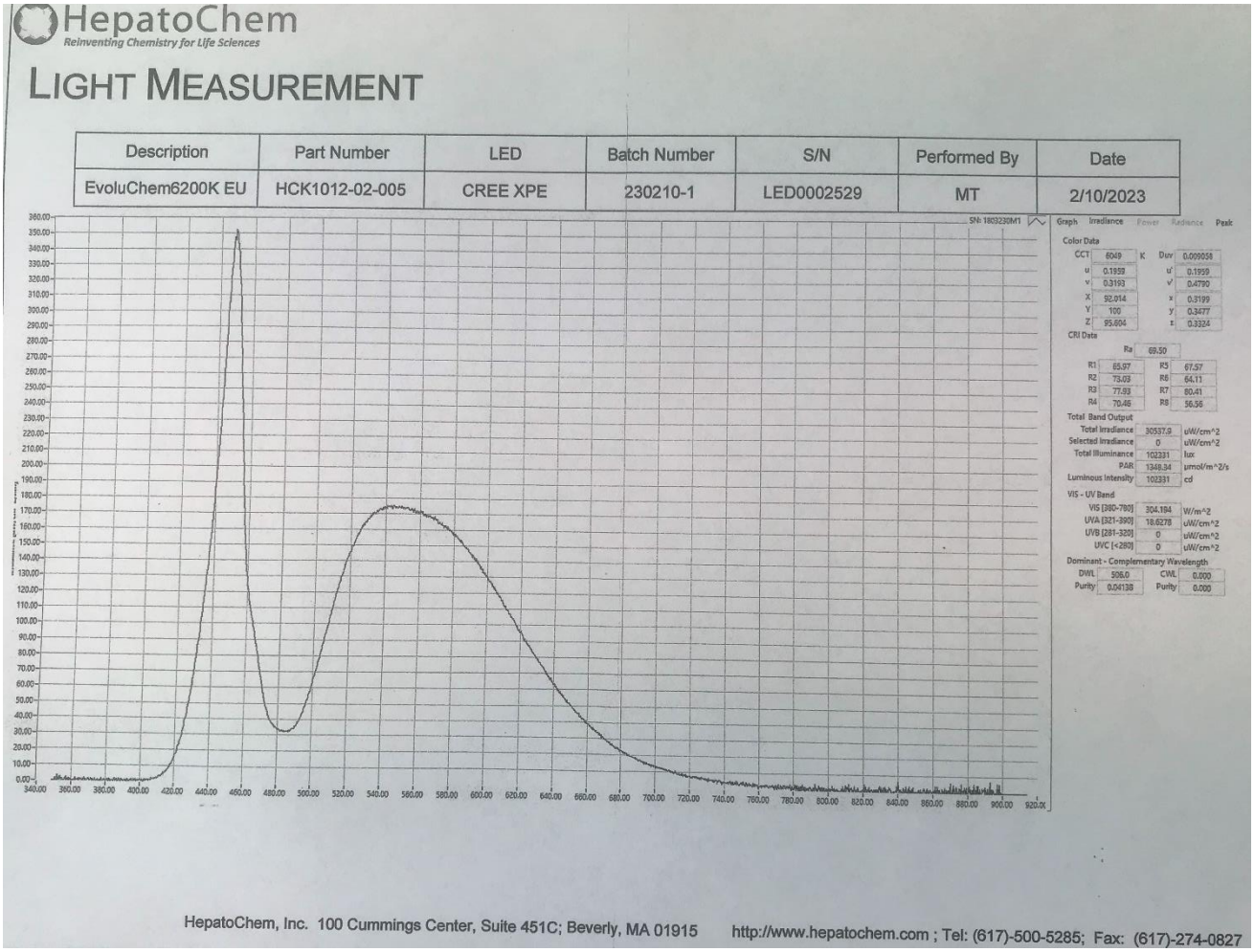

II. Experimental Procedures

Compound 4 :

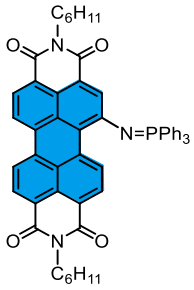

PDI-NO_2 **1** (240 mg, 0.4 mmol) was dissolved in THF / DMF mixture (15 mL; ratio : 1/1) and protected from light, then NaN_3 (31.2 mg, 0.48 mmol) was added. The mixture was stirred at room temperature for 3h until TLC analysis showed complete disappearance of the starting material. To this solution of intermediate azide **3**, PPh_3 (524.6 mg, 2.0 mmol) was added and the mixture was stirred for 48h. The solvent was removed under vacuum and the crude material was extracted using $CHCl_3$ - water mixture. The organic phase was dried over $MgSO_4$ then concentrated and the residue was purified by silica gel chromatography using $CHCl_3$ (100%) then $CHCl_3$ (98%) - ethyl acetate (2%) as the eluents. After precipitation in methanol, a blue-green powder was obtained (226 mg, yield: 68%).

PDI-NO_2 **1** (599 mg, 1 mmol) was dissolved in THF / DMF mixture (40 mL; ratio : 1/1) and protected from light, then NaN_3 (98 mg, 1.5 mmol) and PPh_3 (1.31 g, 5.0 mmol) were added. The mixture was stirred at room temperature for 72h. The solvent was removed under vacuum and the residue was purified by silica gel chromatography using $CHCl_3$ (100%) then $CHCl_3$ (98%) - ethyl acetate (2%) as the eluents. After precipitation in methanol, a blue-green powder was obtained (655 mg, yield: 79%).

^{1}H NMR (500 MHz, $CDCl_3$, 293 K), δ : 10.83 (d, J_{H-H} = 8.5 Hz, 1H), 8.59 (d, J_{H-H} = 8.1 Hz, 1H), 8.51 (d, J_{H-H} = 8.1 Hz, 1H), 8.50 (d, J_{H-H} = 8.3 Hz, 1H), 8.46 (d, J_{H-H} = 8.2 Hz, 1H), 8.32 (d, J = 8.1 Hz, 1H), 7.99 (d, $^4J_{H-P}$ = 1.6 Hz, 1H), 7.90 - 7.86 (m, 6H), 7.67- 7.63 (m, 3H), 7.60 – 7.56 (m, 6H), 5.09 (tt, J_{H-H} = 12.1, 3.7 Hz, 1H, C**H** cyclohexyl), 4.87 (tt, J_{H-H} = 12.1, 3.7 Hz, 1H, C**H** cyclohexyl), 2.68 - 2.56 (m, 2H, CH-C**H$_2$** cyclohexyl), 2.50 - 2.42 (m, 2H, CH-C**H$_2$** cyclohexyl), 2.02 - 1.62 (m, 10H, C**H$_2$** cyclohexyl), 1.55 - 1.23 (m, 6H, C**H$_2$** cyclohexyl).

^{13}C NMR (125 MHz, $CDCl_3$, 293 K), δ: 164.8, 164.7, 164.6, 164.1, 137.9, 135.7, 132.1, 132.9, 132.8, 132.8, 132.6, 131.8, 130.6, 130.5, 130.4, 129.6, 129.5, 129.5, 129.4, 129.3, 129.3, 128.7, 127.6, 126.4, 126.2, 123.5, 123.3, 123.2, 122.7, 122.5, 122.1, 120.5, 120.1, 53.8, 53.8, 29.3, 29.2, 26.8, 26.7, 25.7, 25.6 ppm.

^{31}P NMR (202.4 MHz, $CDCl_3$, 293 K, δ : 9.74.

HR-MS (MALDI-TOF, DCTB, negative mode) m/z = calc for $C_{54}H_{44}N_4O_7P$: 829.3069; found 829.3075 (0.77 ppm error).

λ,nm (ε, L.mol^{-1}.cm^{-1}) in CH_2Cl_2: 639 (42 200), 600 (36 500), 470 (5 500), 430 (20 800).

Compound 5 :

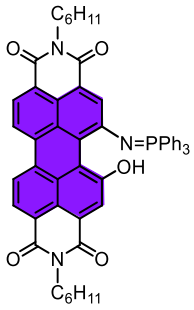

A solution of PDI-NO_2 (599 mg, 1 mmol) and PPh_3 (865 mg, 3.3 mmol) in anhydrous THF (100 mL) in a round-bottom flask was irradiated under white LED lamp for two hours and controlled by TLC ($CHCl_3$/ethyl acetate: 96/4). The solution was concentrated then the crude material was purified by silica gel chromatography using CH_2Cl_2 then CH_2Cl_2/EtOAc (90/10) as the mixture of eluents. After precipitation in methanol, a dark-violet powder was obtained (795 mg, yield: 94%).

The same reaction carried out in CH_2Cl_2 yielded 794 mg (94% yield) of compound **5**.

^{1}H NMR (500 MHz, $CDCl_3$, 293 K, δ): 12.72 (s, 1H), 8.53 (s, 2H), 8.50 (s, 2H), 8.41 (s, 1H), 8.09 (d, $^4J_{H\text{-}H}$ = 1.3 Hz, 1H), 7.75 – 7.69 (m, 6H), 7.65 – 7.60 (m, 3H), 7.55 – 7.50 (m, 6H), 5.09 (tt, $J_{H\text{-}H}$ = 12.2, 3.8 Hz, 1H, CH cyclohexyl), 4.92 (tt, $J_{H\text{-}H}$ = 12.2, 3.8 Hz, 1H, CH cyclohexyl), 2.63 (qd, $J_{H\text{-}H}$ = 12.2, 3.6 Hz, 2H, CH-C**H$_2$** cyclohexyl), 2.49 (qd, $J_{H\text{-}H}$ = 12.4, 3.6 Hz, 2H, CH-C**H$_2$** cyclohexyl), 1.99 – 1.62 (m, 11H, CH_2 cyclohexyl), 1.54 – 1.20 (m, 5H, CH_2 cyclohexyl) ppm.

^{13}C NMR (125 MHz, $CDCl_3$, 293 K, δ): 165.0, 164.7, 164.7, 164.2, 158.5, 144.1, 144.0, 133.7, 133.6, 133.6, 133.1, 133.0, 129.7, 129.6, 129.4, 128.8, 128.7, 128.6, 127.9, 127.8, 127.7, 127.2, 126.7, 125.9, 124.2, 124.0, 123.8, 122.7, 122.1, 122.0, 121.9, 121.3, 53.9, 53.8, 29.4, 29.2, 26.8, 26.7, 25.7, 25.6 ppm.

^{31}P NMR (202.4 MHz, $CDCl_3$, 293 K, δ): 20.23 ppm.

HR-MS (MALDI, DCTB, positive mode) m/z $[M]^{\bullet+}$ calc for $[C_{54}H_{44}N_3O_5P]^{\bullet+}$: 845.3022; found 845.3013.

λ,nm (ε, L.mol^{-1}.cm^{-1}) in CH_2Cl_2: 594 (44 800), 556 (33 000), 429 (13 800).

Compound 6 :

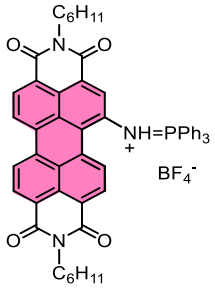

To a solution of 82.9 mg (0.1 mmol) of compound **4** in anhydrous CH_2Cl_2 (10 mL) was added $HBF_4.Et_2O$ 50-55% in Et_2O (0.1 mL). After stirring for 5 min at room temperature, petroleum ether was added for the precipitation of compound **6**. The precipitate was filtered, washed with petroleum ether, dried under vacuum affording compound **6** in quantitative yield (91 mg).

^{1}H NMR (500 MHz, $CDCl_3$, 293 K, δ): 9.28 (d, $J_{H\text{-}H}$ = 8 Hz, 1H), 8.69 (br.s, 1H), 8.56 (d, $J_{H\text{-}H}$ = 8 Hz, 1H), 8.50 (d, $J_{H\text{-}H}$ = 8 Hz, 1H), 8.42-8.39 (m, 3H), 8.36 (d, $J_{H\text{-}H}$ = 8 Hz, 1H), 7.61-7.57 (m, 9H), 7.48-7.45 (m, 6H), 5.00 (t, $J_{H\text{-}H}$ = 12.2 Hz, 1H, C**H** cyclohexyl), 4.90 (t, $J_{H\text{-}H}$ = 12.2 Hz, 1H, C**H** cyclohexyl), 2.55 (dq, $J_{H\text{-}H}$ = 12.2, 3.6 Hz, 2H, CH-C**H$_2$** cyclohexyl), 2.46 (dq, $J_{H\text{-}H}$ = 12.4, 3.6 Hz, 2H, CH-C**H$_2$** cyclohexyl), 1.94 – 1.87 (m, 4H, C**H$_2$** cyclohexyl), 1.80 – 1.70 (m, 6H, C**H$_2$** cyclohexyl), 1.50-1.25 (m, 6H, C**H$_2$** cyclohexyl) ppm.

^{13}C NMR (125 MHz, $CDCl_3$, 293 K, δ): 163.9, 163.6, 163.5, 162.5, 135.6, 135.5, 134.1, 133.8, 133.7, 133.4, 133.3, 133.27, 133.2, 132.9, 131.2, 130.4, 130.2, 130.1, 129.0, 128.6, 127.8, 127.5, 126.5, 124.1, 124.0, 123.6, 123.5, 123.1, 119.7, 119.0, 54.3, 29.4, 29.1, 26.7, 26.6, 25.6, 25.5 ppm.

^{31}P NMR (202.4 MHz, $CDCl_3$, 293 K, δ): 39.09 ppm.

^{19}F NMR (283 MHz, $CDCl_3$, 293 K, δ): - 149.63 ppm.

Compound 7 :

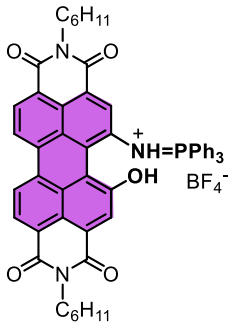

To a solution of 84.5 mg (0.1 mmol) of compound **5** in anhydrous CH_2Cl_2 (10 mL) was added $HBF_4.Et_2O$ 50-55% in Et_2O (0.1 mL). After stirring for 5 min at room temperature, petroleum ether was added for the precipitation of compound **7**. The precipitate was filtered, washed with petroleum ether, dried under vacuum affording compound **7** in quantitative yield (93 mg).

The ^{1}H NMR spectrum clearly shows the presence of two isomeric forms. However, a single peak is present in the ^{31}P spectrum, suggesting effectively the presence of a single compound.

^{31}P NMR (202.4 MHz, $CDCl_3$, 293 K, δ): 34.06 ppm.

III. Characterizations

1. NMR spectra

Compound 4 :

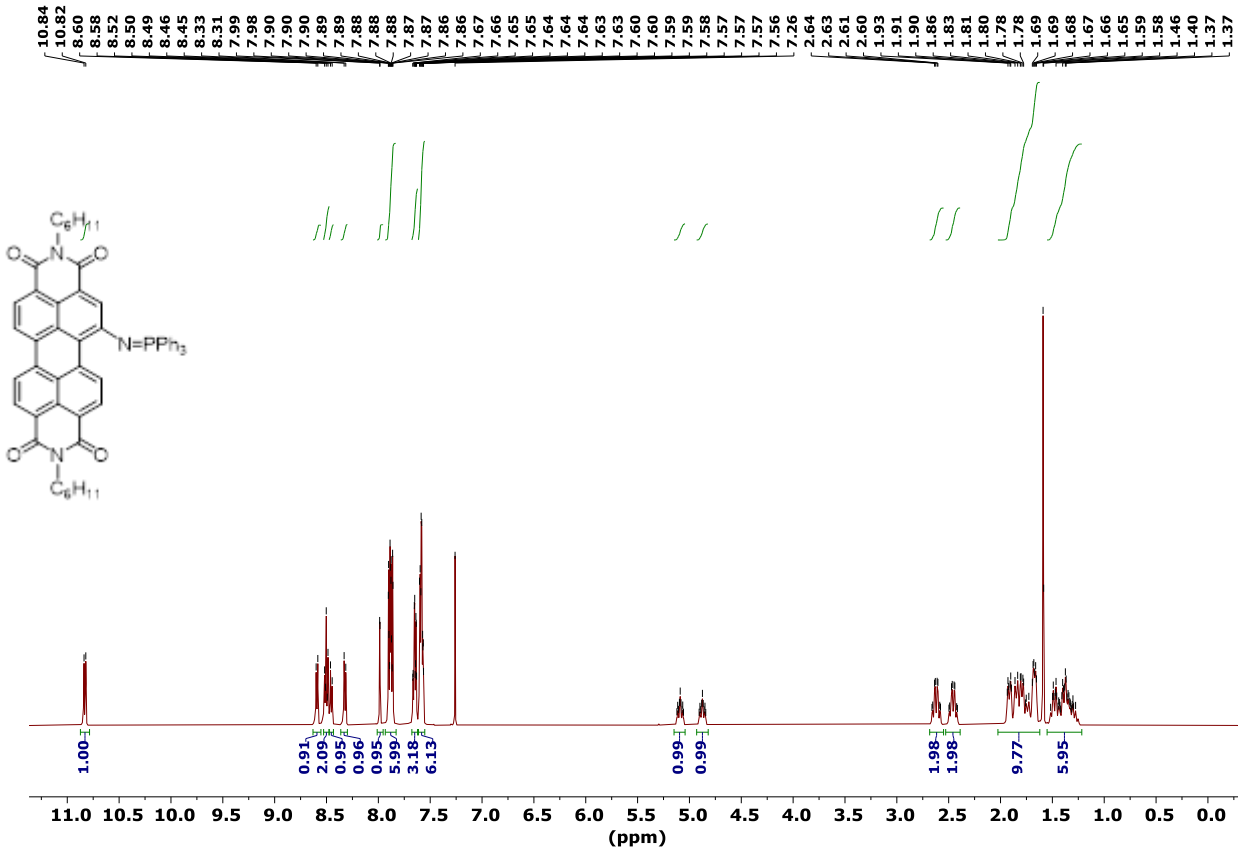

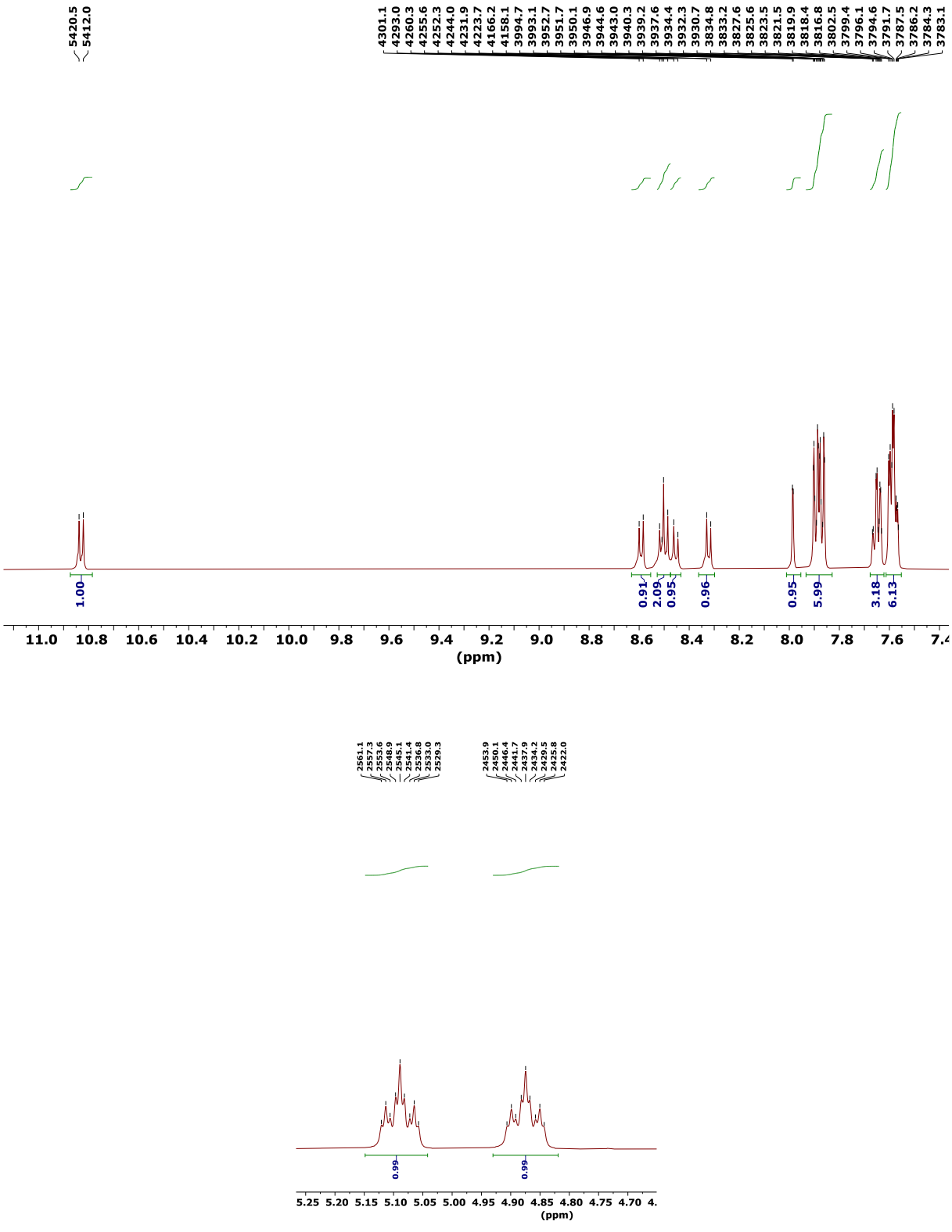

*Figure S1: ^{1}H NMR (500 MHz, $CDCl_3$, 293 K) of compound **4**, enlargement of the aromatic region and protons of both cyclohexyl groups.*

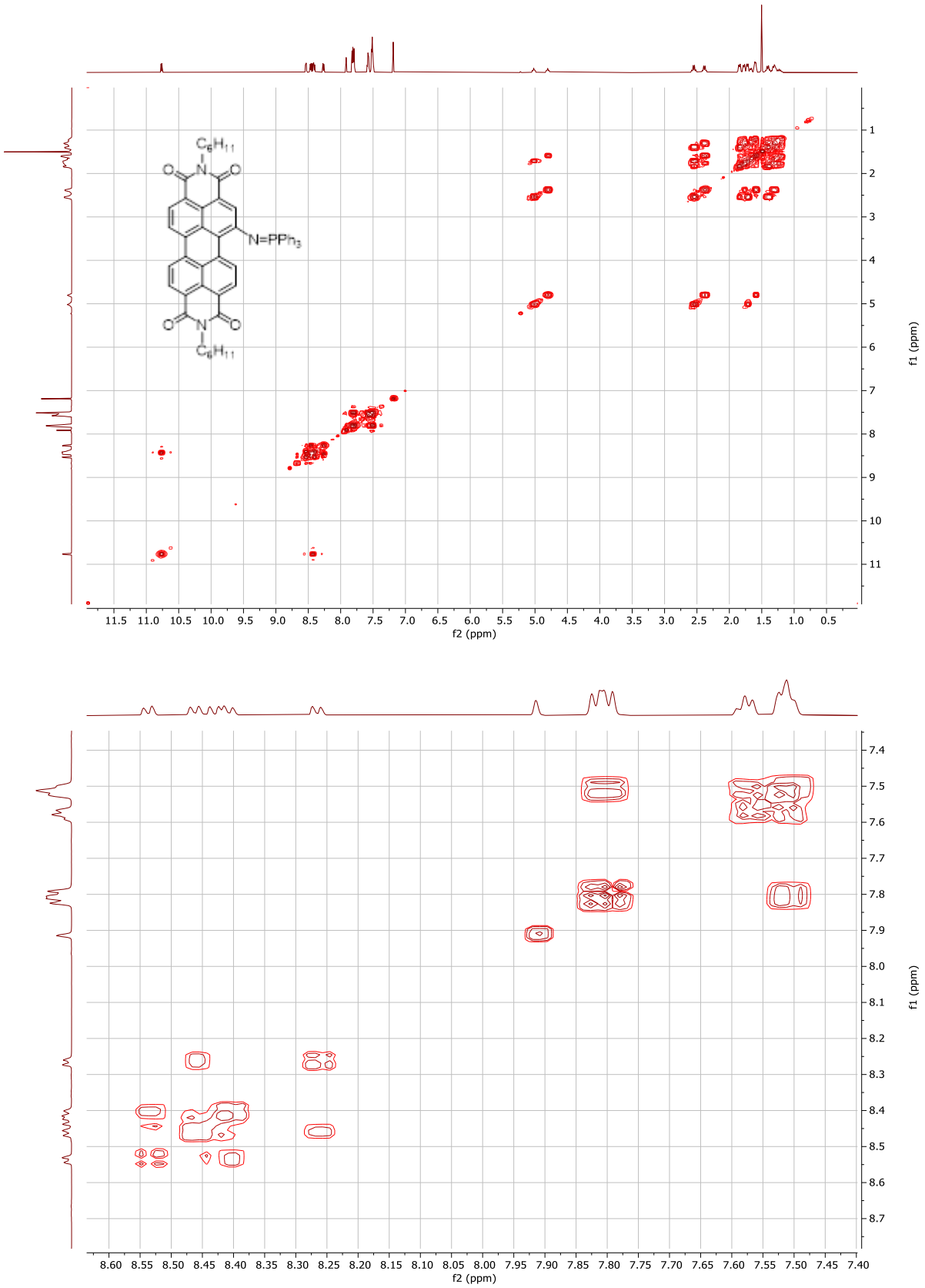

*Figure S2: 2D ^{1}H NMR (500 MHz, $CDCl_3$, 293 K) of compound **4** and enlargement of the aromatic region.*

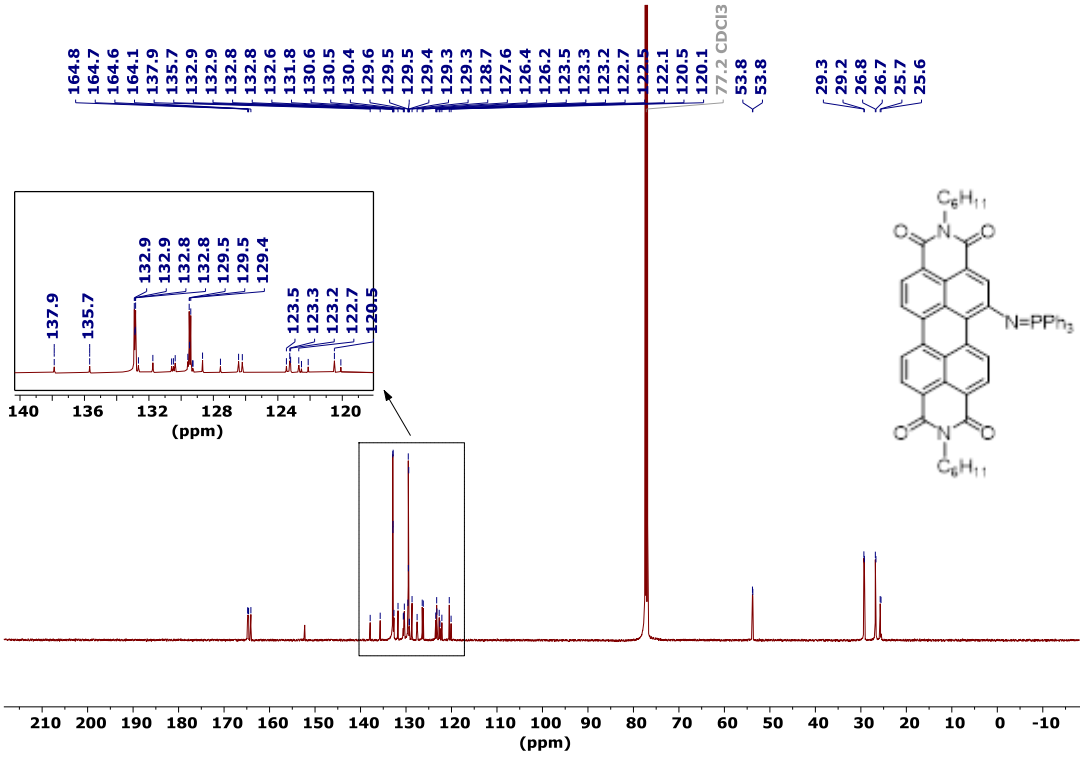

*Figure S3: ^{13}C NMR (125 MHz, $CDCl_3$, 293 K) of compound **4**.*

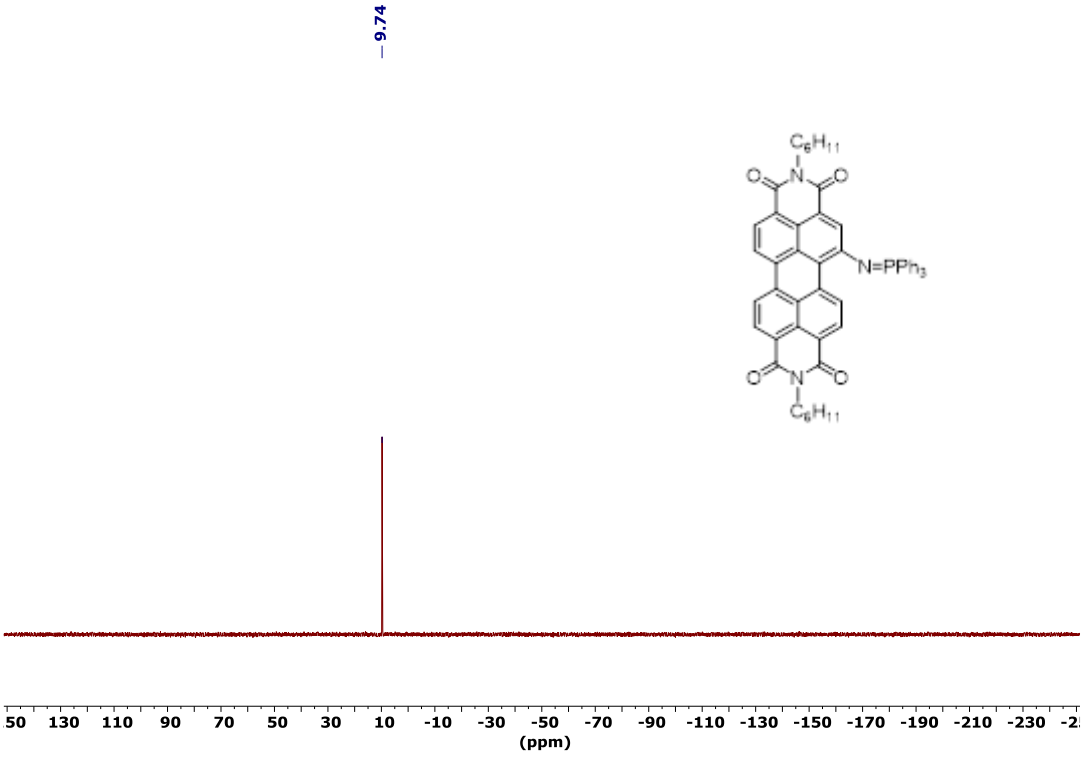

*Figure S4: ^{31}P NMR (202.4 MHz, $CDCl_3$, 293 K) of compound **4**.*

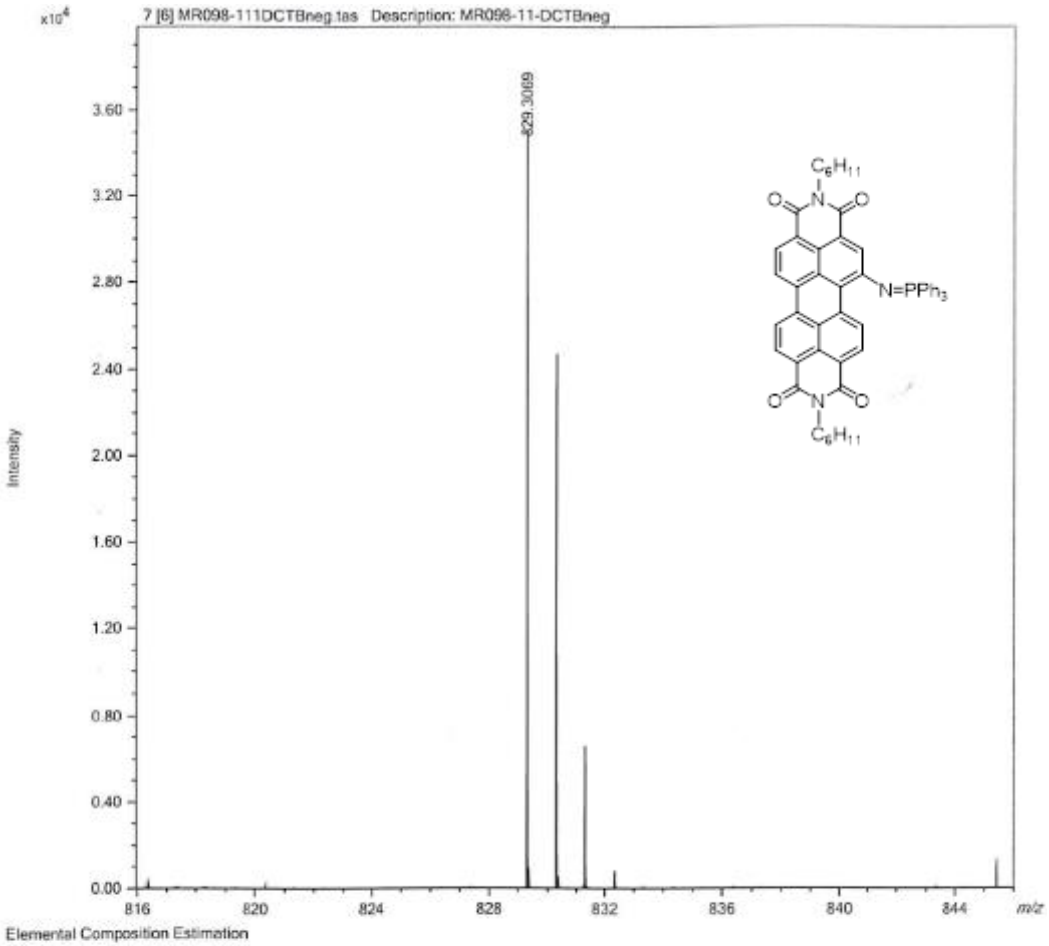

Elemental Composition Estimation

Parameters:

Mass	Tolerance	Electron Mode	Charge	DBE Range	Max Results
829.30685 ± 0.00166	2.0 ppm	Odd	1	-0.5 - 200.0	100

Elements

C 0 - 60 H 0 - 50 O 0 - 5 N 0 - 5 P 1 - 1

Results:

#	Formula	Mass	DBE	Abs. Error (u)	Error (u)	Error (ppm)
1	C54 H44 N3 O4 P	829.30749	35.0	0.00064	-0.00064	-0.77

*Figure S5: HR-MS (MALDI-TOF, DCTB matrix) of compound **4**.*

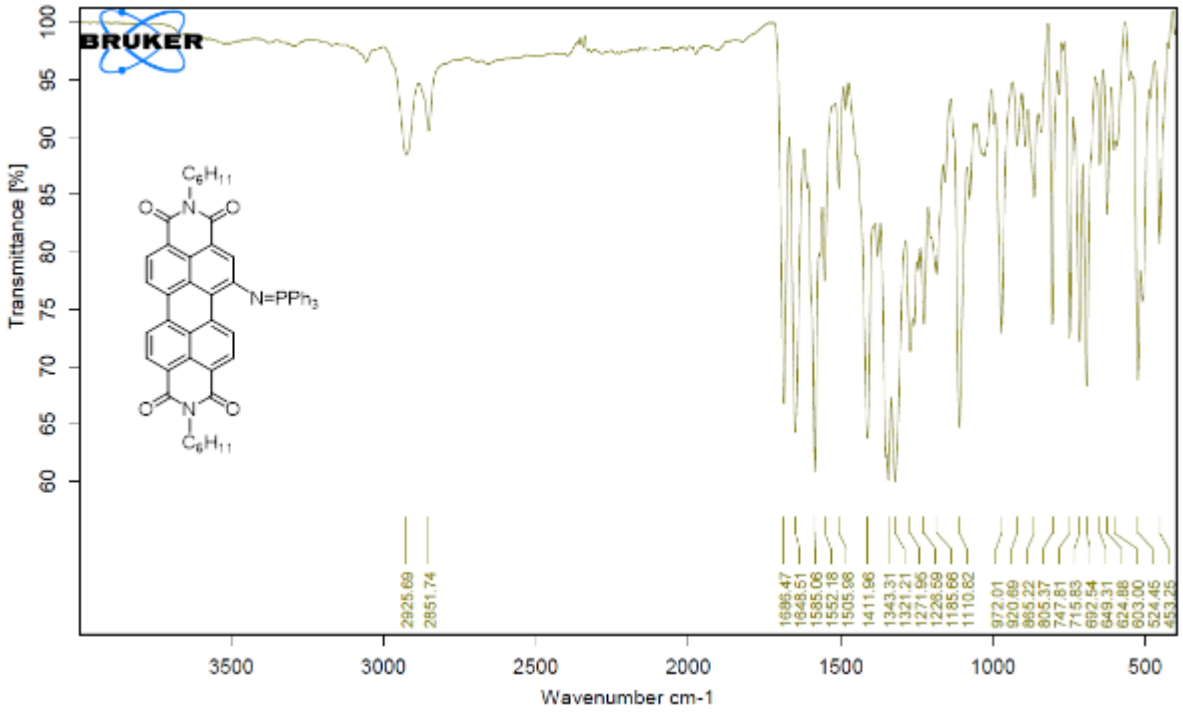

*Figure S6: FT-IR spectrum of compound **4**.*

Compound 5 :

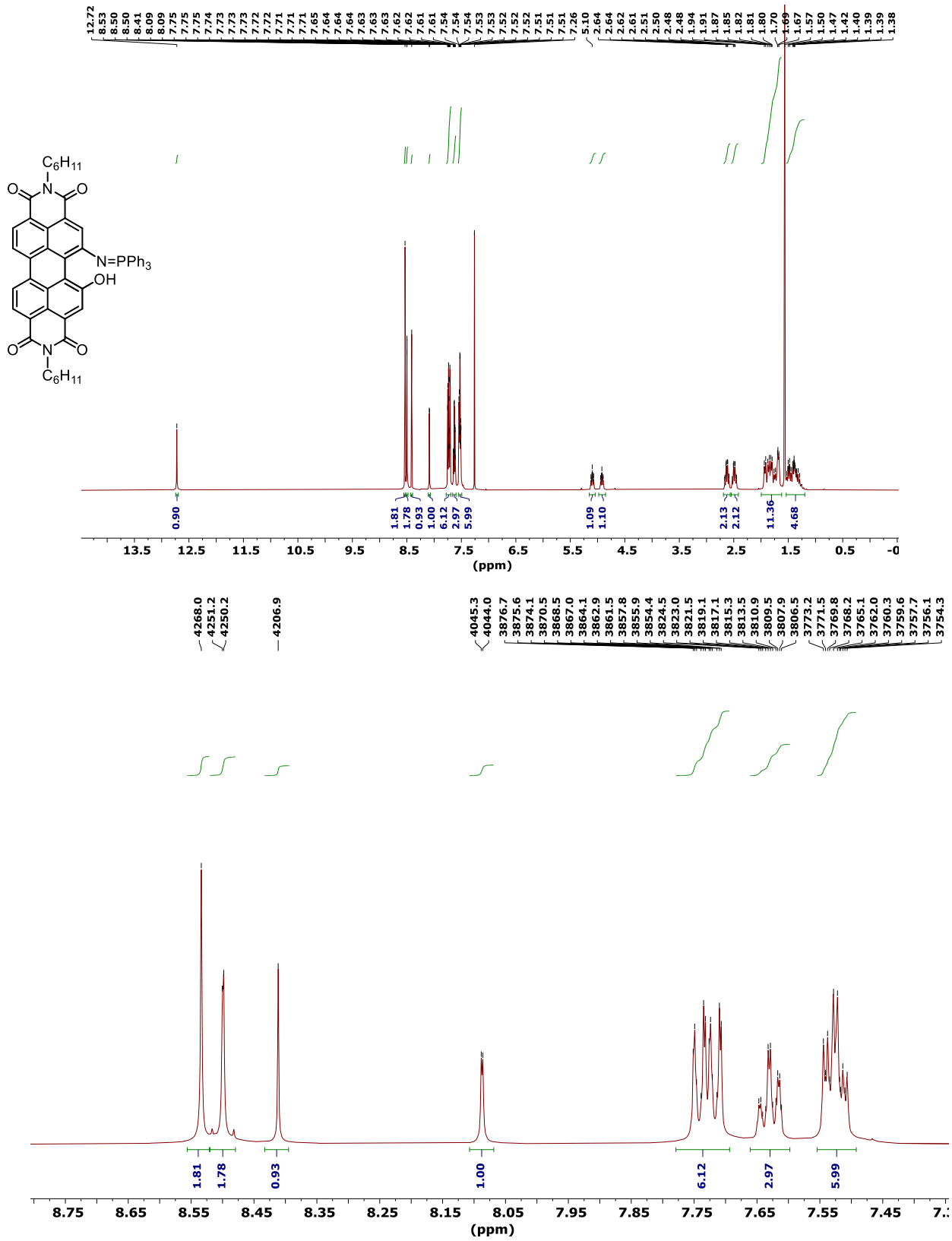

*Figure S7: ^{1}H NMR (500 MHz, $CDCl_3$, 293 K) of compound **5** and enlargement of the aromatic region.*

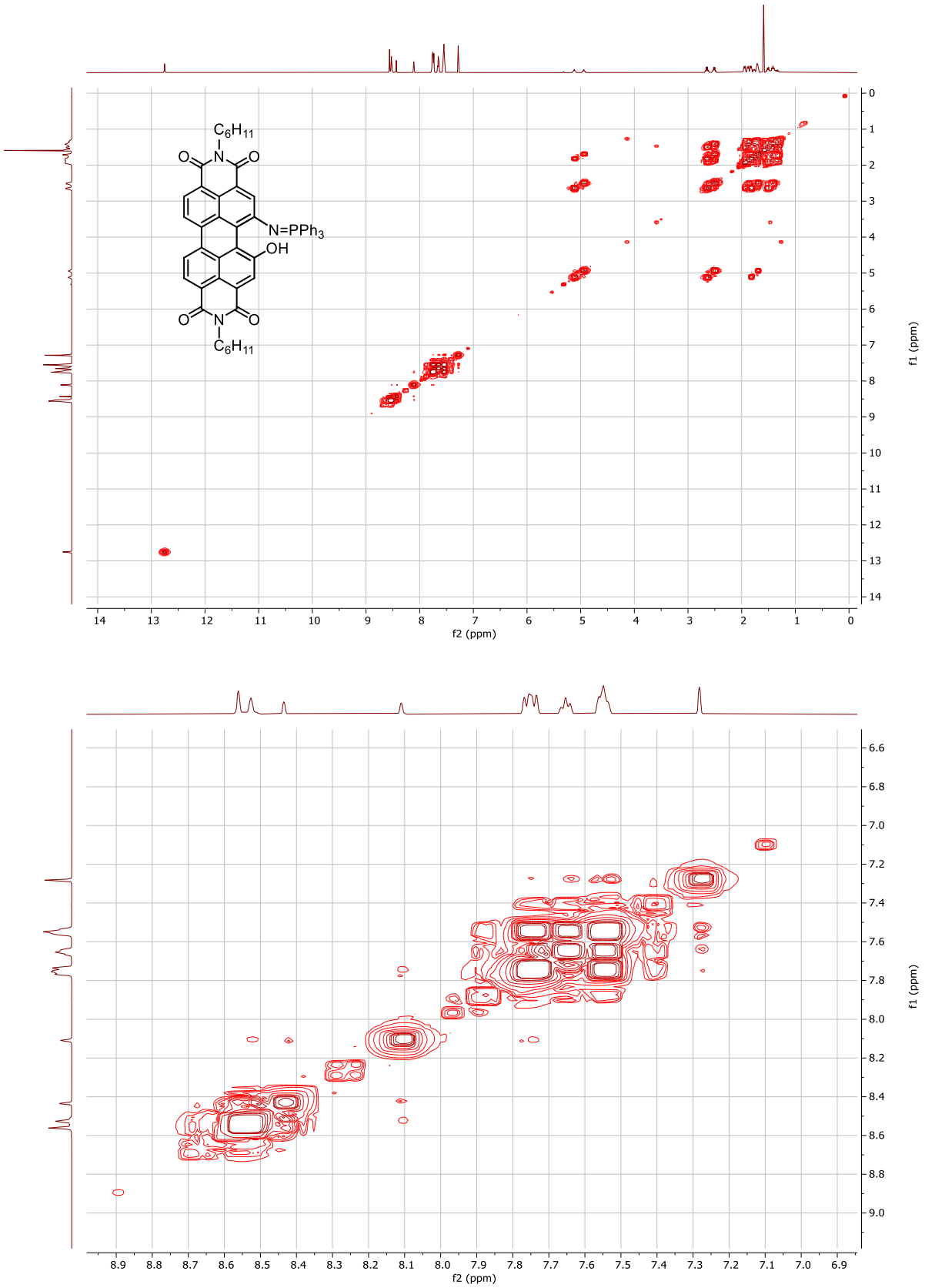

*Figure S8: 2D ^{1}H NMR (500 MHz, $CDCl_3$, 293 K) of compound **5** and enlargement of the aromatic region.*

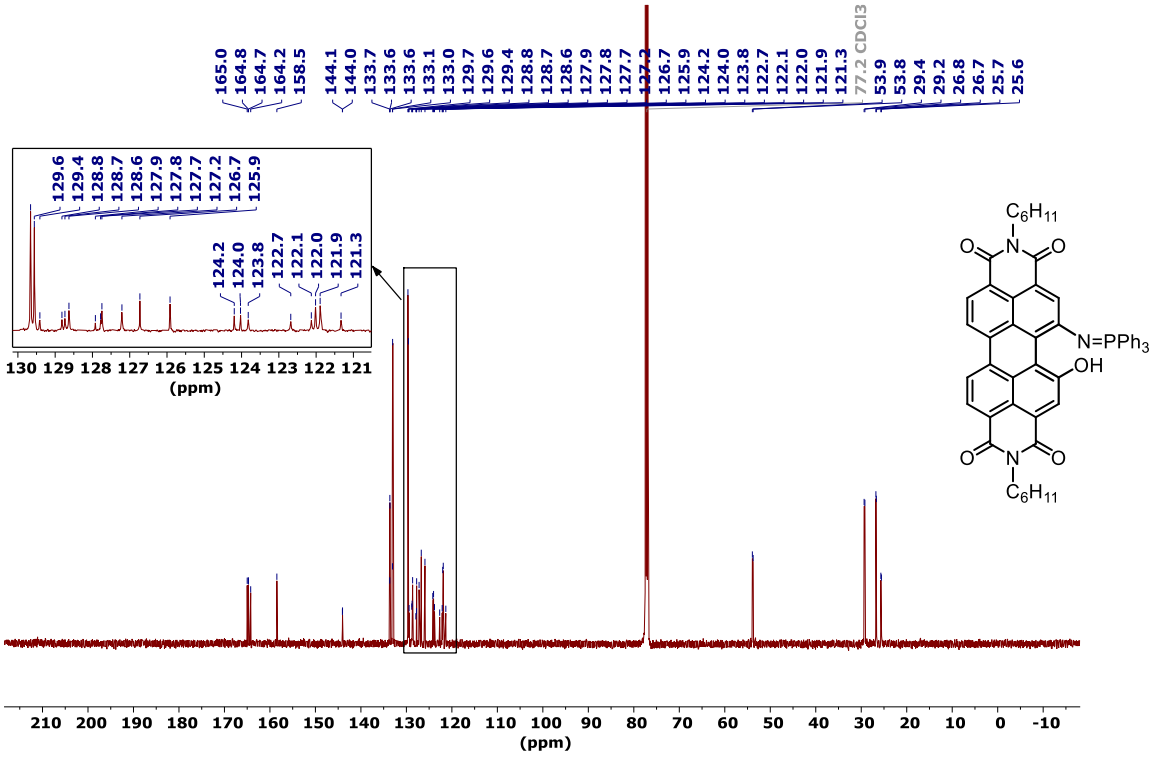

*Figure S9: ^{13}C NMR (125 MHz, $CDCl_3$, 293 K) of compound **5**.*

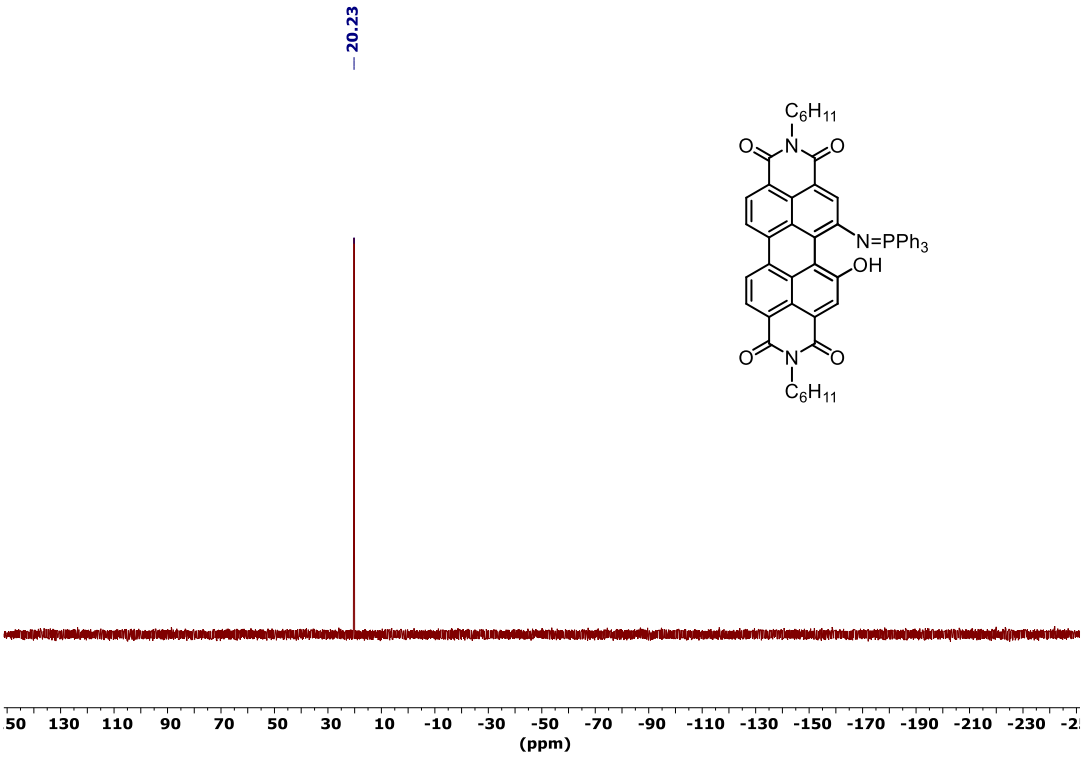

*Figure S10: ^{31}P NMR (202.4 MHz, $CDCl_3$, 293 K) of compound **5**.*

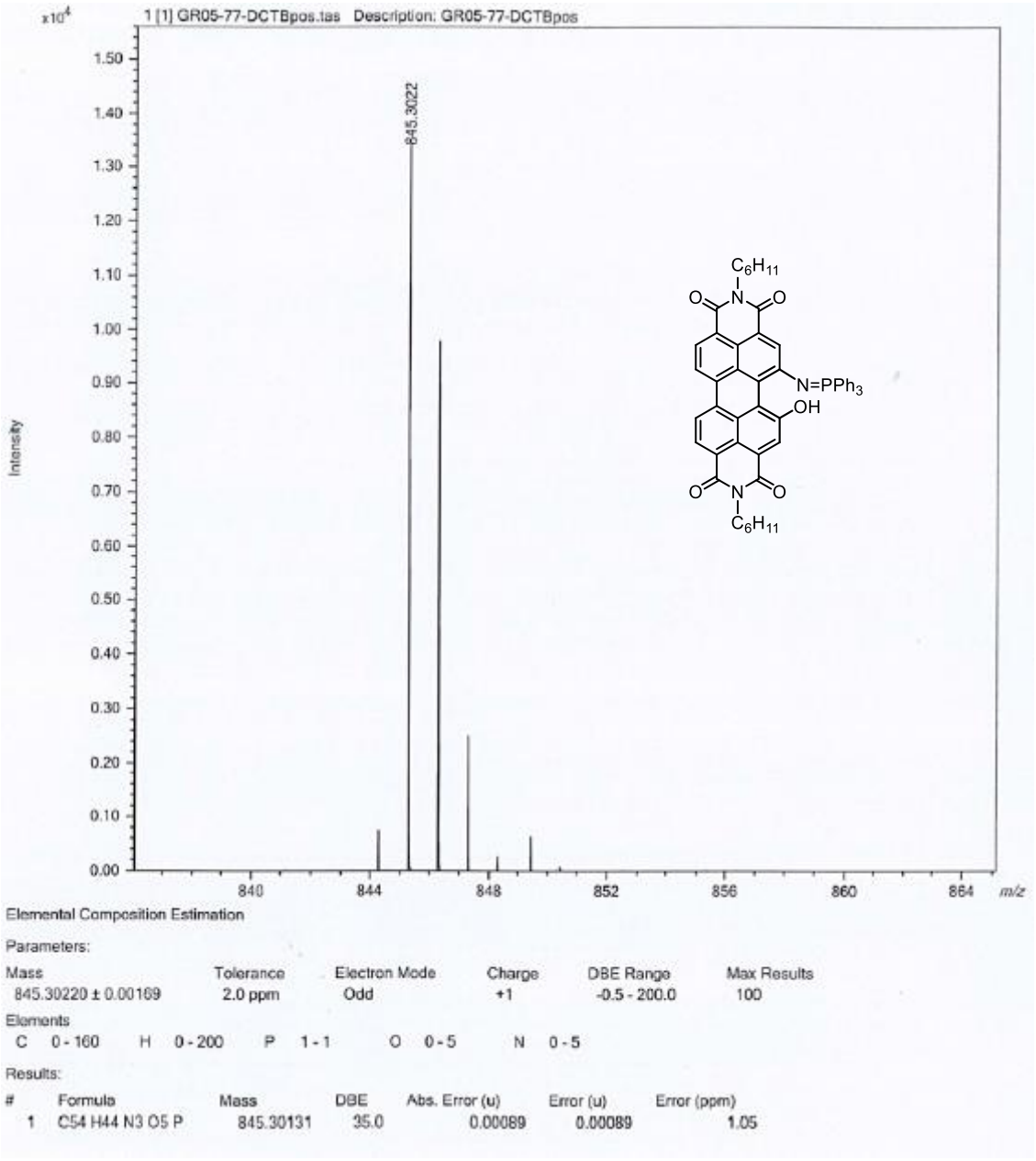

*Figure S11: HR-MS (MALDI, DCTB matrix) of compound **5**.*

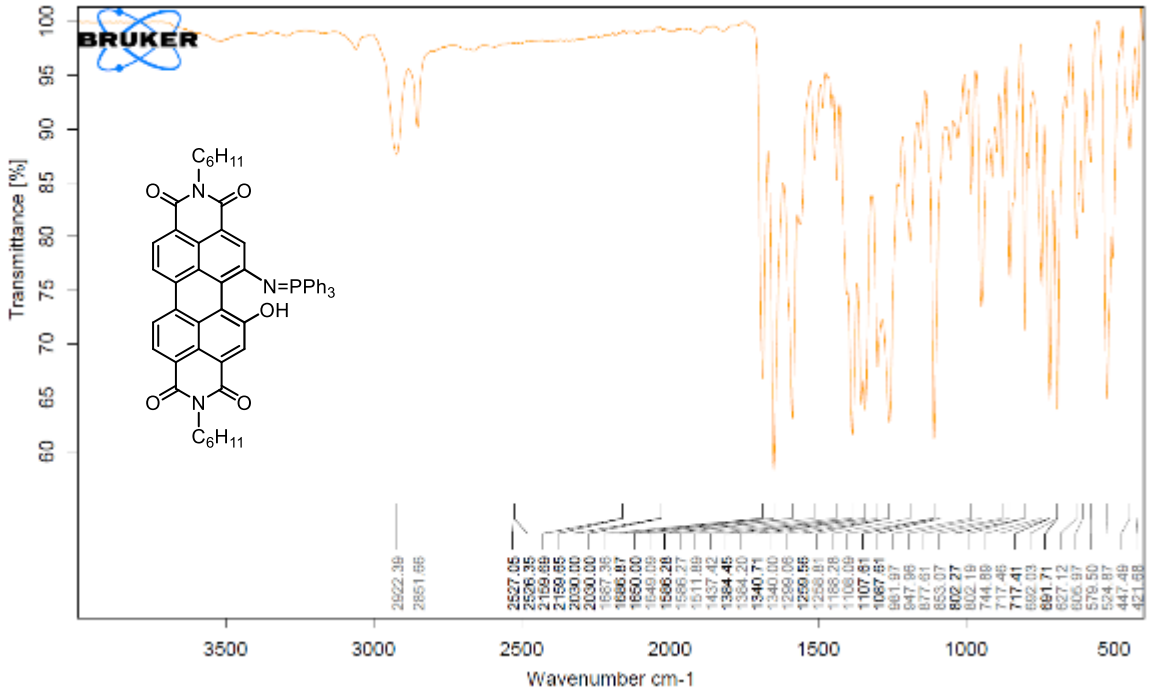

*Figure S12: FT-IR spectrum of compound **5**.*

Compound 6 :

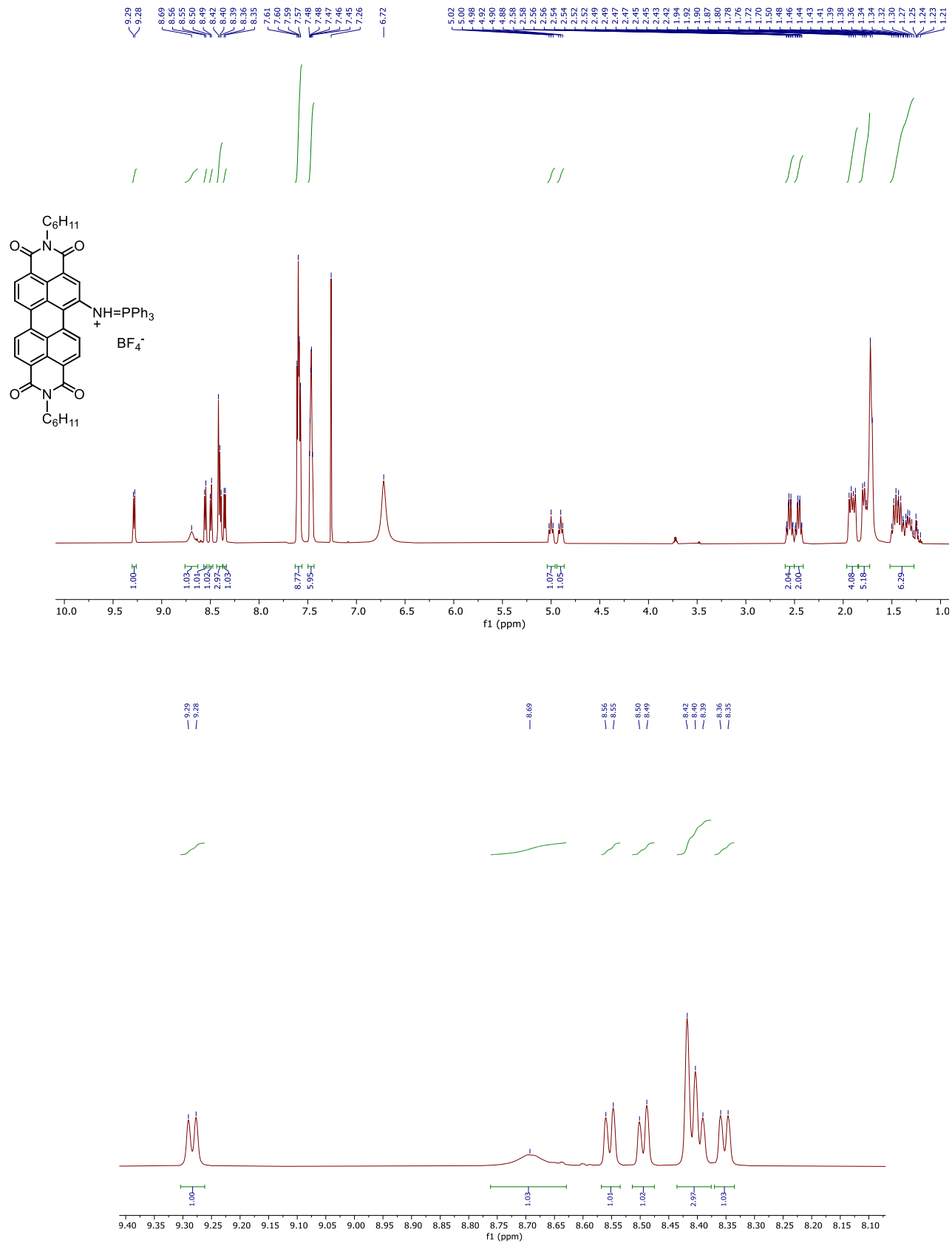

*Figure S13: ^{1}H NMR (500 MHz, $CDCl_3$, 293 K) of compound **6**.*

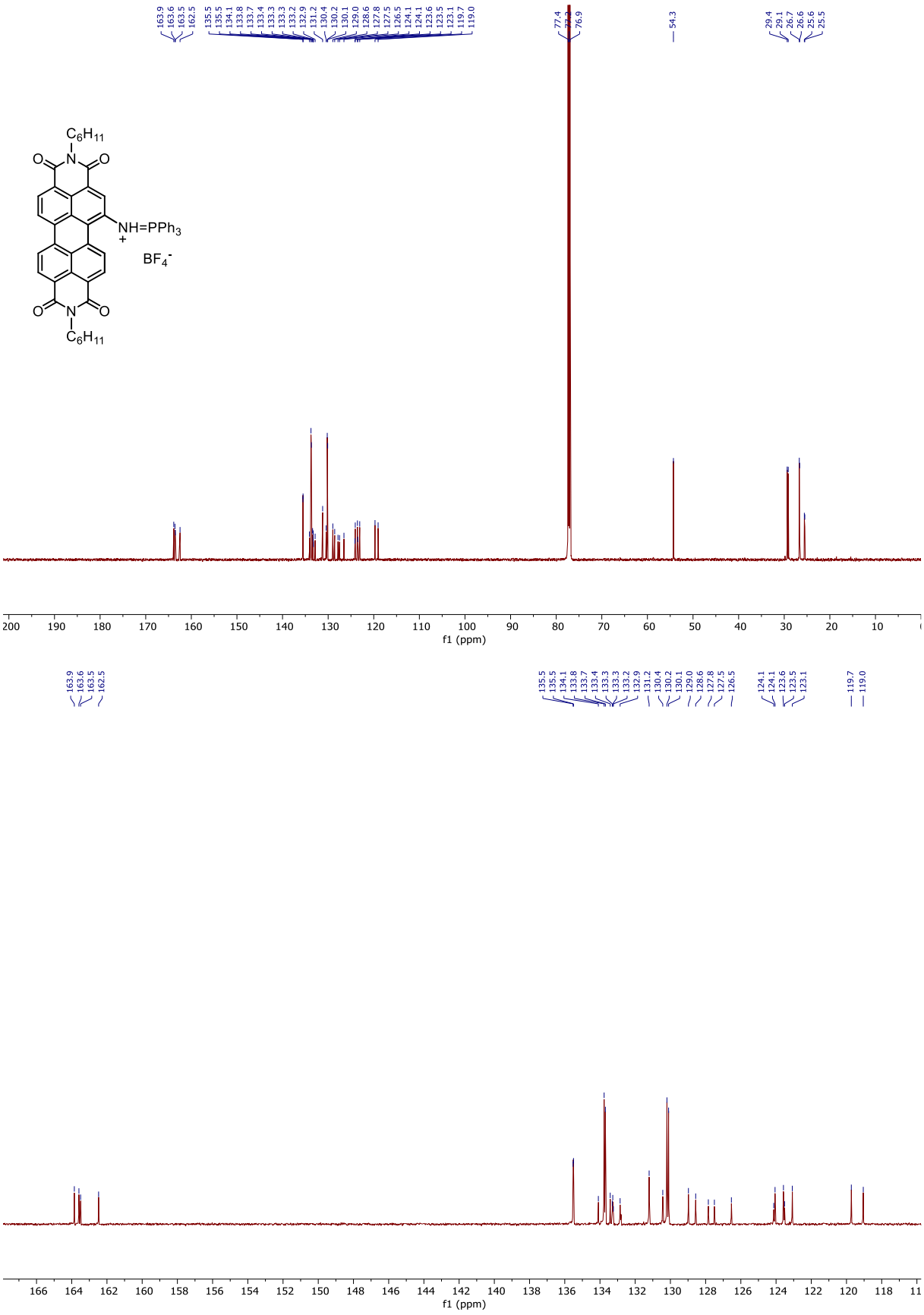

*Figure S14: ^{13}C NMR (125 MHz, $CDCl_3$, 293 K) of compound **6**.*

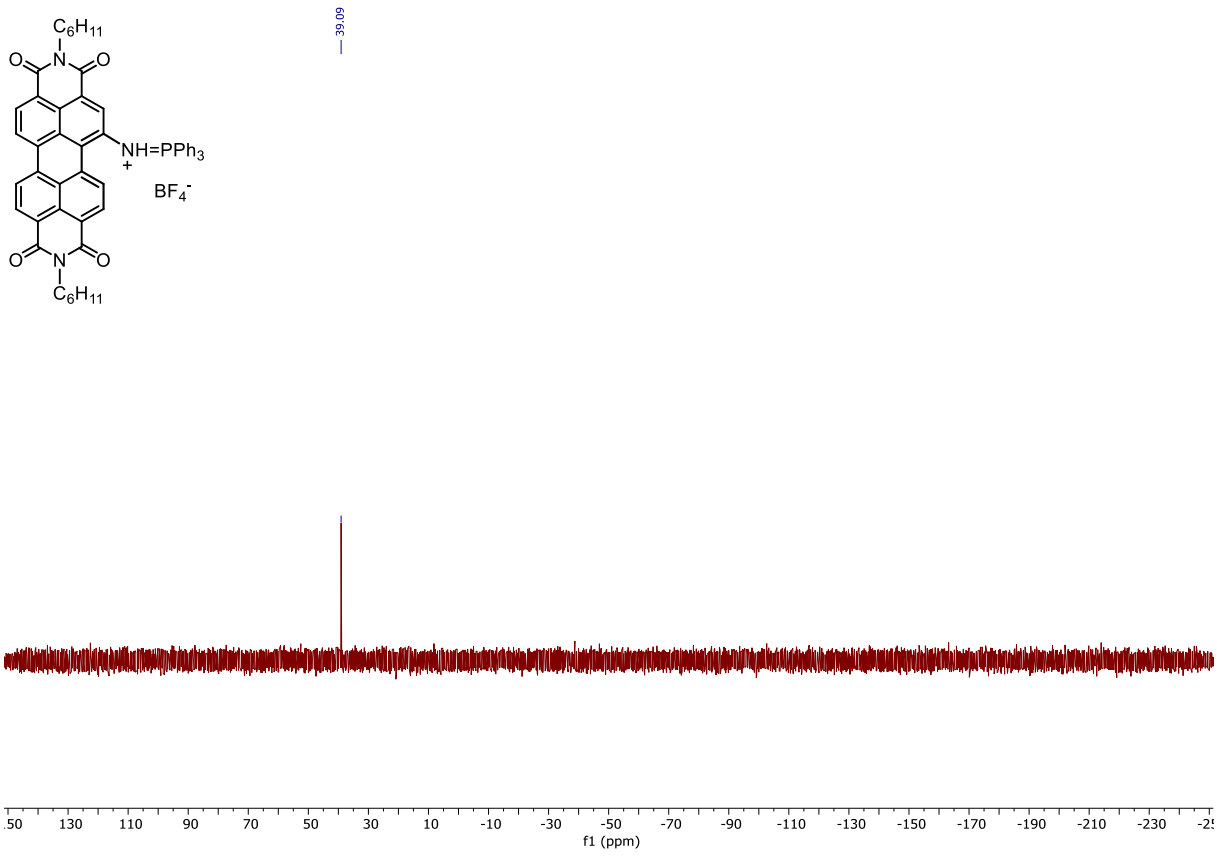

*Figure S15: ^{31}P NMR (202.4 MHz, $CDCl_3$, 293 K) of compound **6**.*

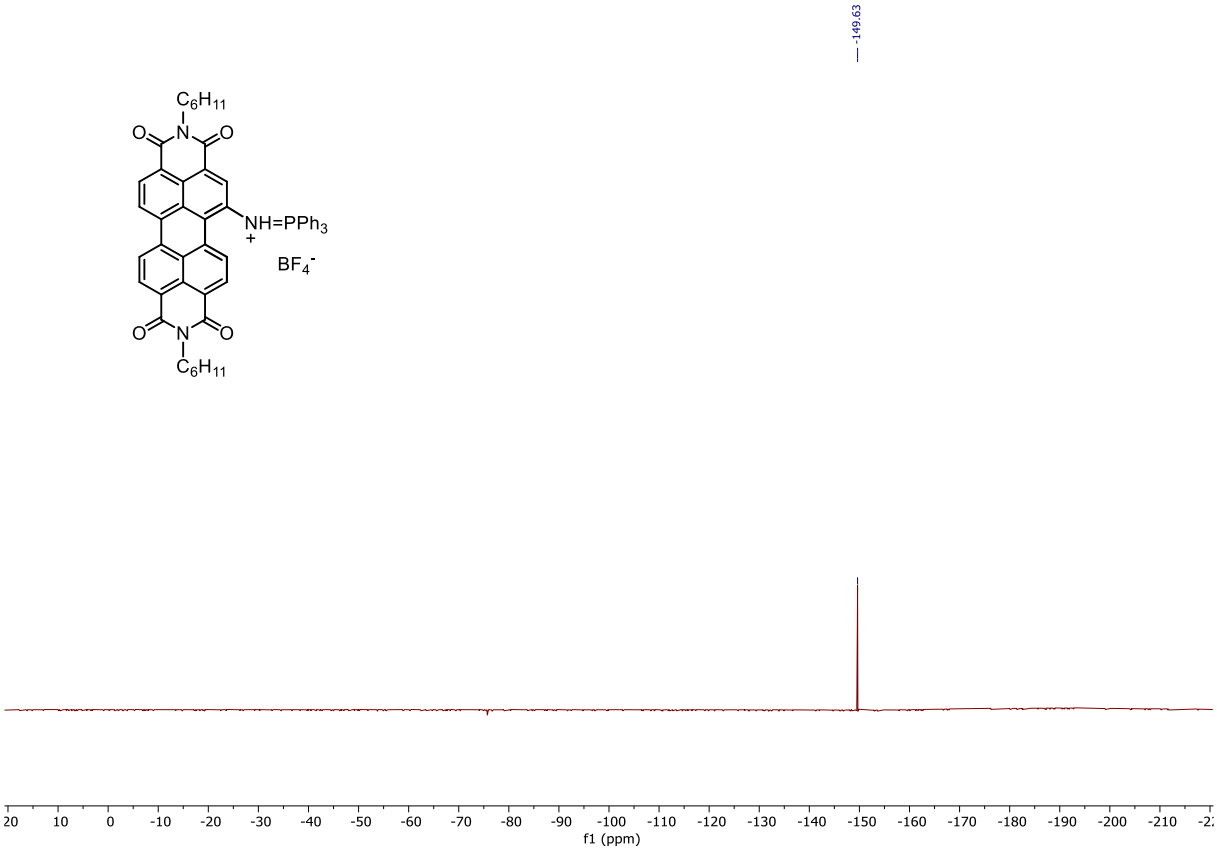

*Figure S16: ^{19}F NMR (283 MHz, $CDCl_3$, 293 K) of compound **6**.*

Compound 7 :

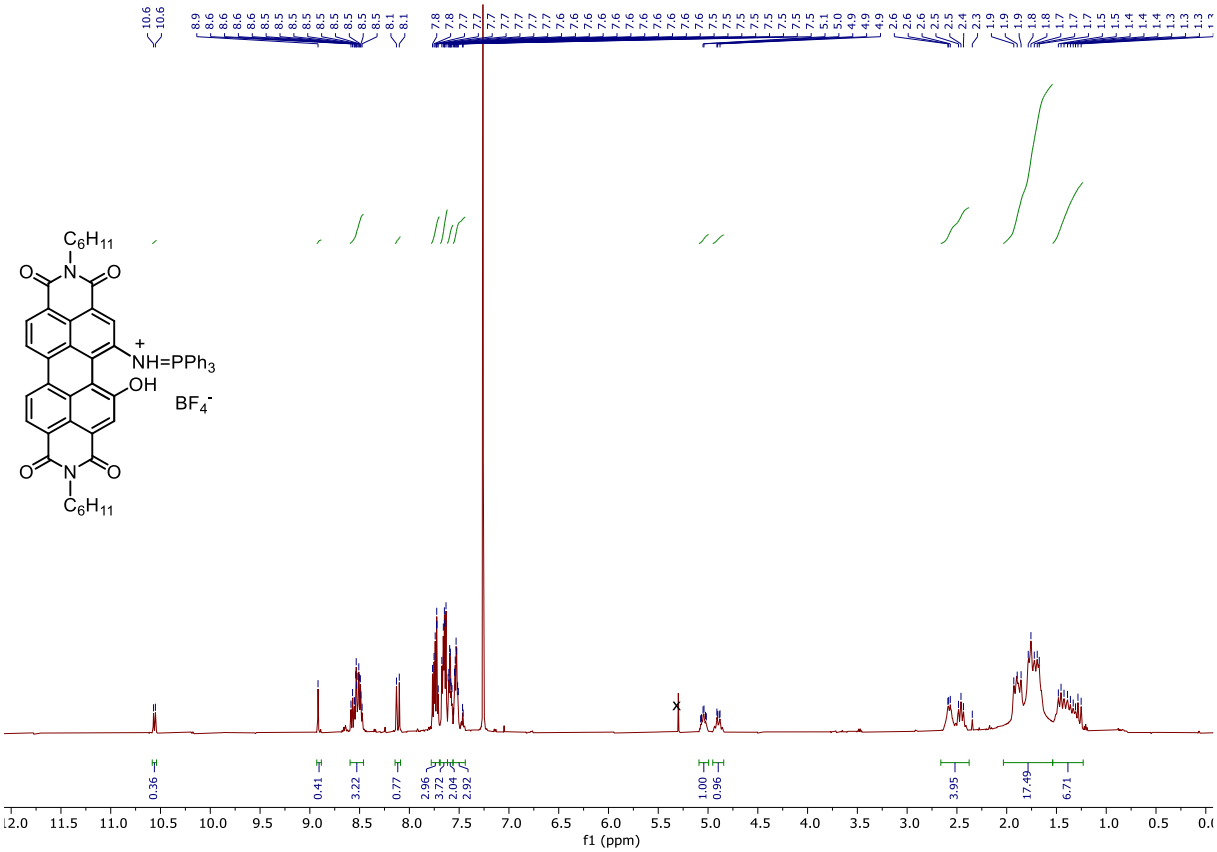

*Figure S17: ^{1}H NMR (500 MHz, $CDCl_3$, 293 K) of compound **7**.*

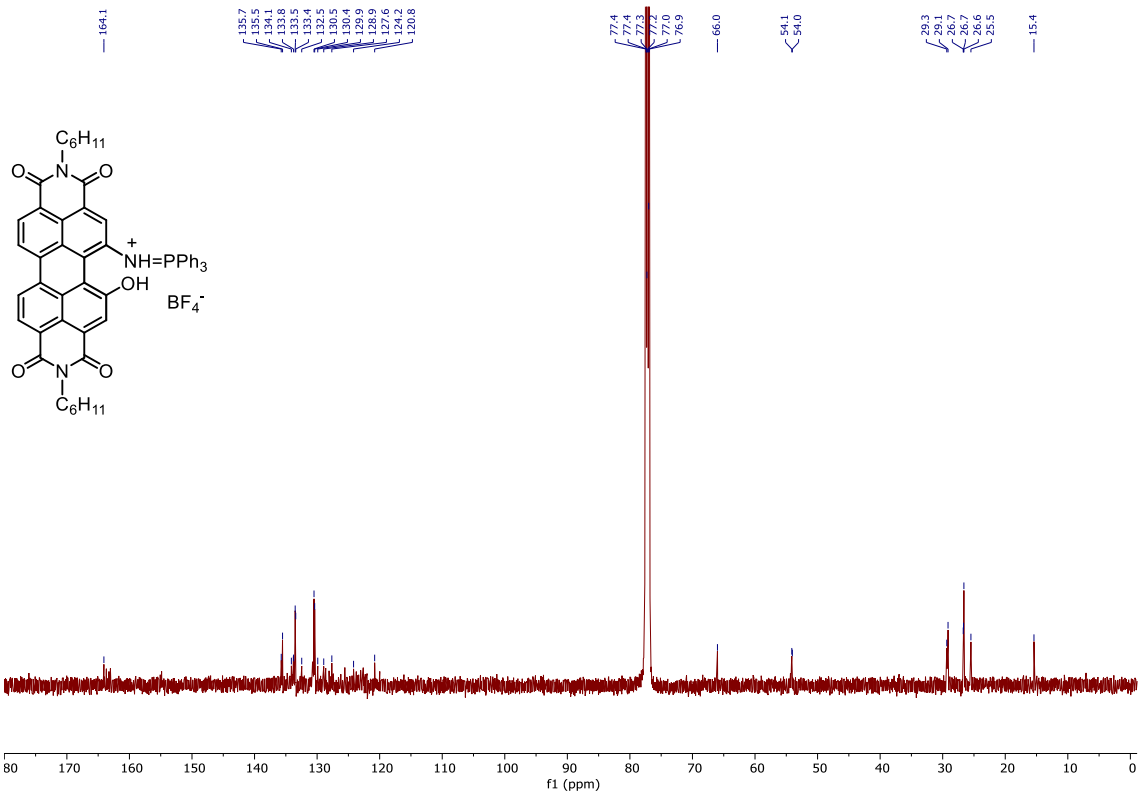

*Figure S18: ^{13}C NMR (125 MHz, $CDCl_3$, 293 K) of compound **7**, poorly soluble in $CDCl_3$.*

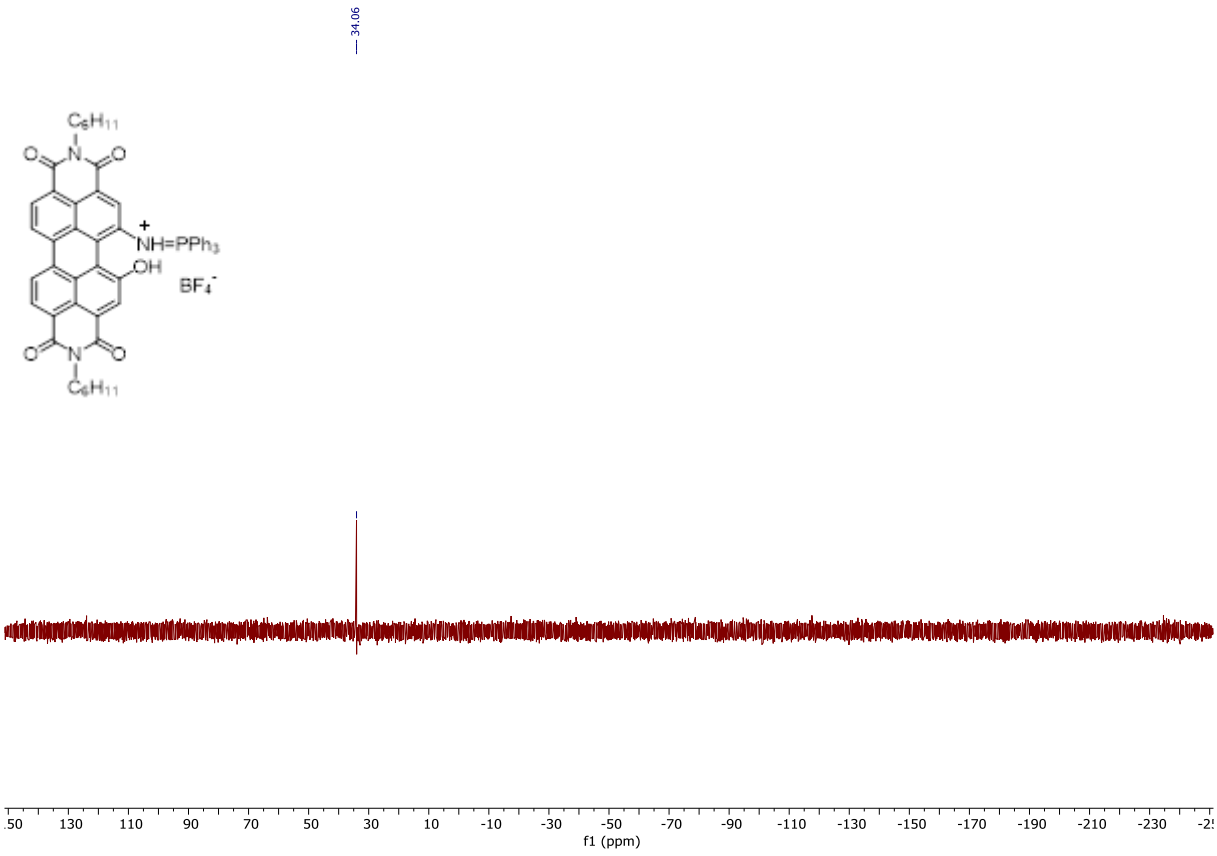

*Figure S19: ^{31}P NMR (202.4 MHz, $CDCl_3$, 293 K) of compound **7**.*

2. Absorption and fluorescence spectroscopies

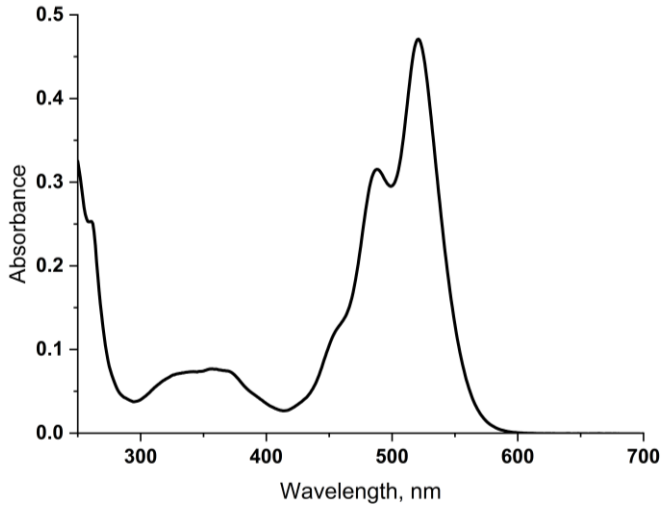

*Figure S20: UV-Visible spectra of nitroPDI **1** in CH_2Cl_2 (10^{-5} M).*

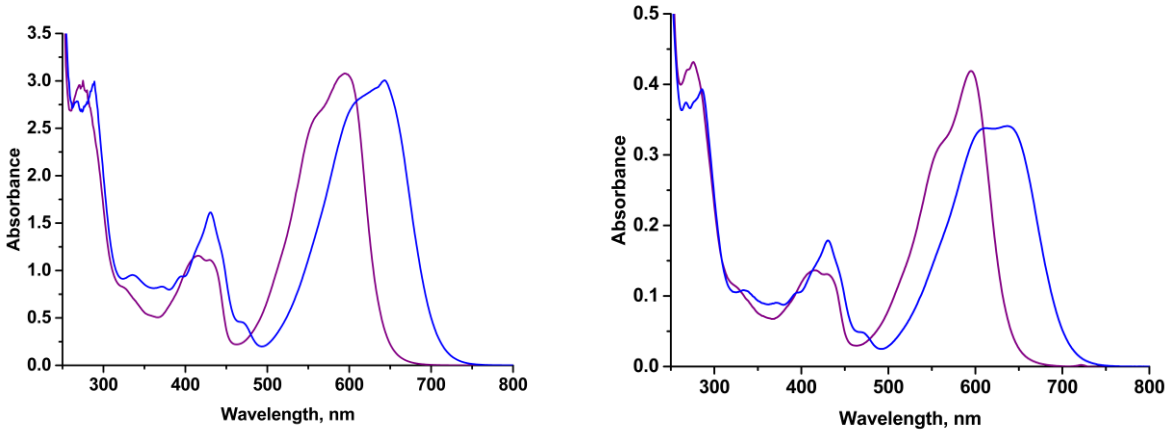

*Figure S21: UV-Visible spectra of compound **4** (blue) and compound **5** (violet) in CH_2Cl_2 at 10^{-4} M (left) and 10^{-5} M (right). Some aggregation can be noticed for compound **4** at higher concentration.*

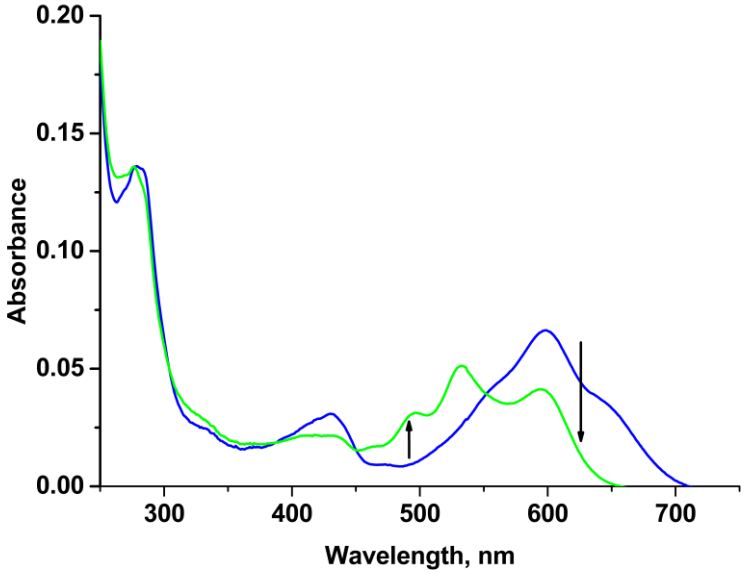

*Figure S22: Photostability study of compound **4** at 10^{-6} M in CH_2Cl_2*
UV-Visible spectra at t = 0 (blue), after 3 h of irradiation with the LED lamp (green).

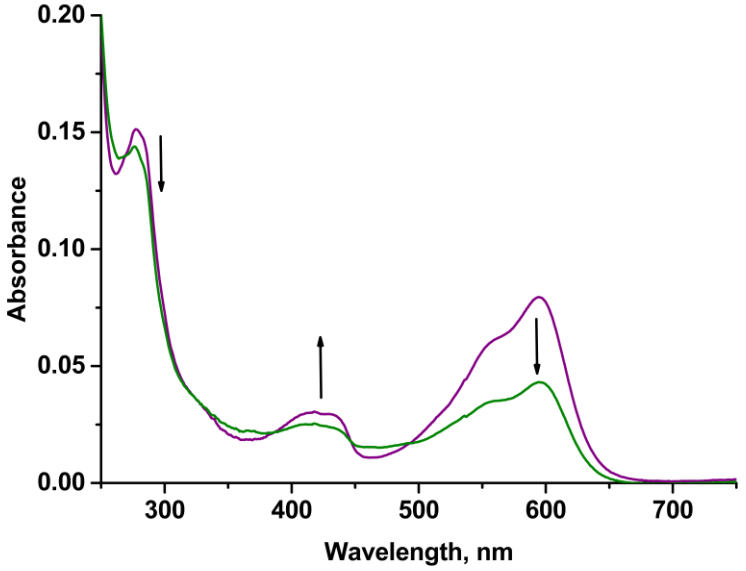

*Figure S23: Photostability study of compound **5** at 10^{-6} M in CH_2Cl_2*
UV-Visible spectra at t = 0 (violet), after 3 h of irradiation with the LED lamp (olive).

3. Electrochemistry

The electrochemical properties of compounds **1**, **4** and **5** were investigated in glove-box in anhydrous dichloromethane at a scan rate of 100 mV s^{-1} using 0.1 M nBu_4NPF_6 in CH_2Cl_2 as supporting electrolyte. Pt électrodes were used as both the working and counter electrodes, and with Ag/AgCl as the pseudoreference electrode. A ferrocene/ferrocenium (Fc/Fc^+) redox couple was used as internal standard and was assigned an absolute energy level of –4.8 eV vs vacuum.

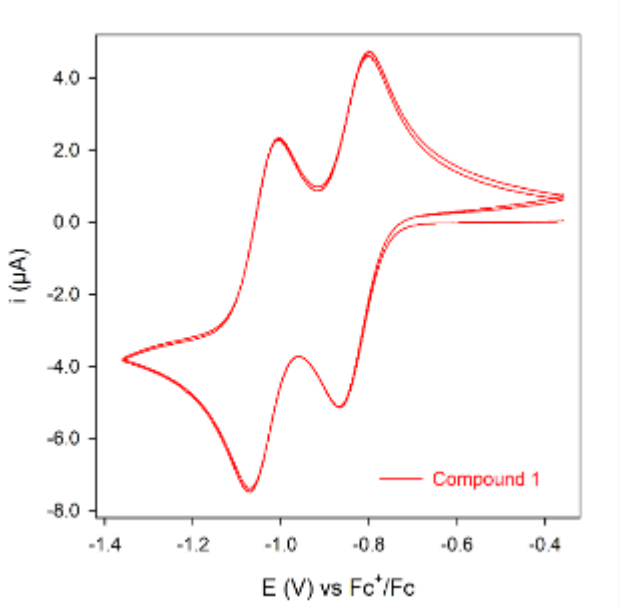

*Figure S24: Cyclic voltammogram of compound **1** ($C = 10^{-3}$ M in CH_2Cl_2).*

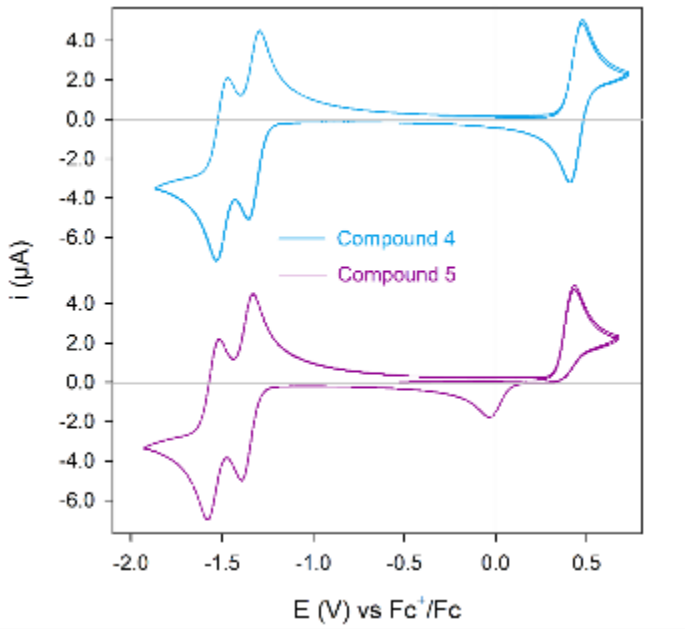

*Figure S25: Cyclic voltammograms of compounds **4** and **5** ($C = 10^{-3}$ M in CH_2Cl_2).*

4. Spectroelectrochemistry

Iminophosphorane-PDI 4:

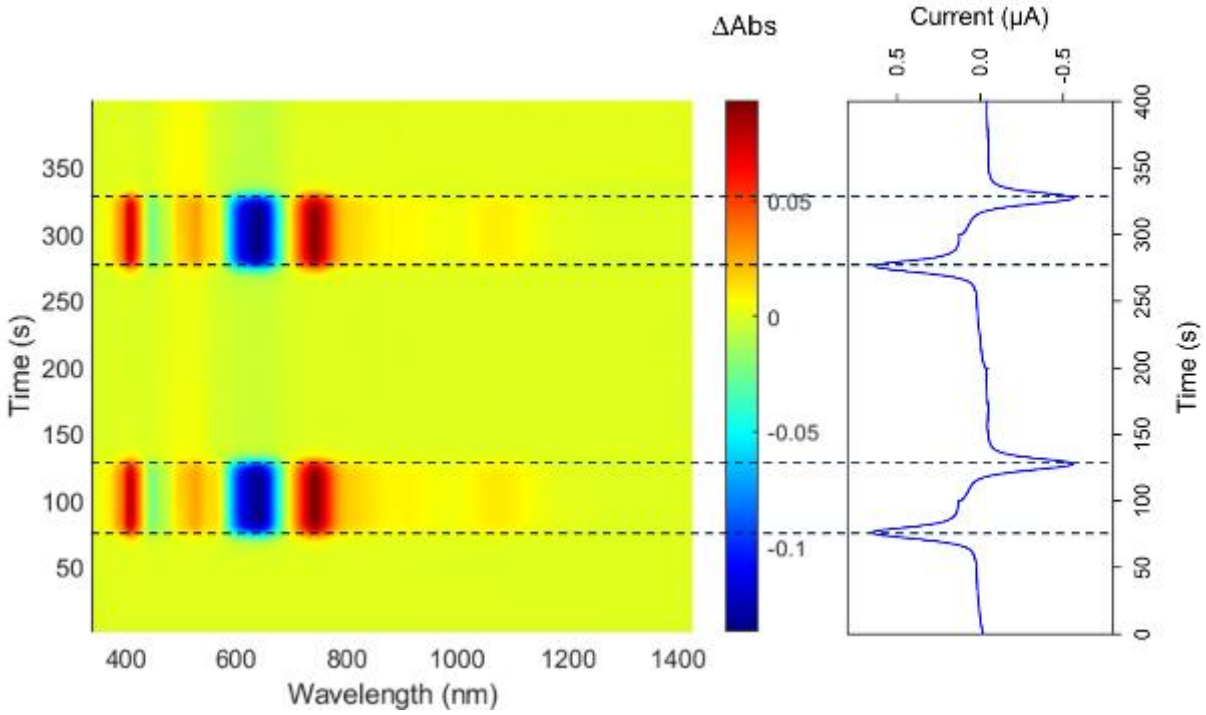

*Figure S26: Absorption variation recorded by real-time absorption spectroelectrochemistry of iminophosphorane-PDI **4** under thin-layer conditions in 1 mM CH_2Cl_2 with n-Bu_4NPF_6 (0.1 M in CH_2Cl_2), using Pt as the working electrode.*

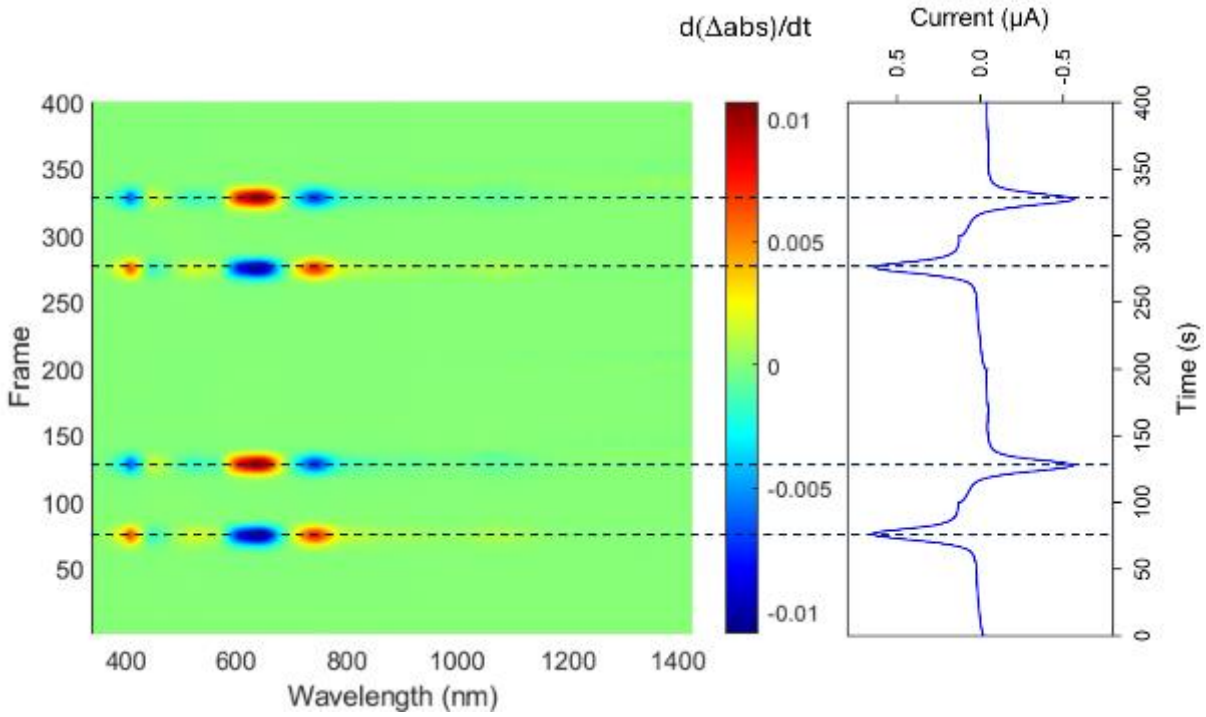

*Figure S27: Absorption variation derivative recorded by real-time absorption spectroelectrochemistry of iminophosphorane-PDI **4** under thin-layer conditions in 1 mM CH_2Cl_2 with n-Bu_4NPF_6 (0.1 M in CH_2Cl_2), using Pt as the working electrode.*

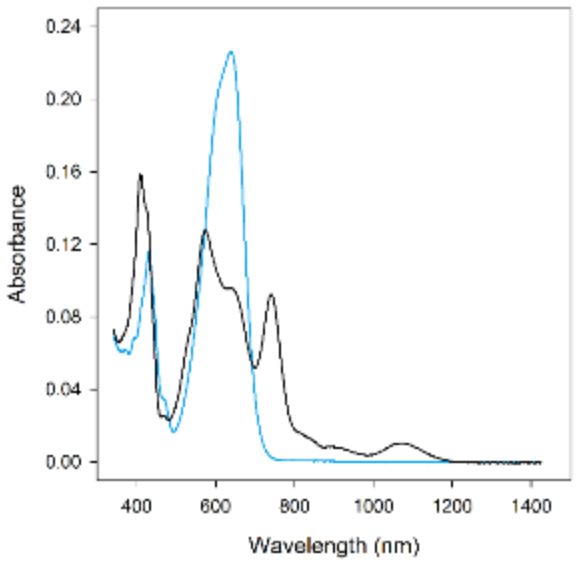

*Figure S28: Absorption spectra of iminophosphorane-PDI **4** in neutral state (blue) and in oxidized state (black).*

Iminophosphorane-PDI 5:

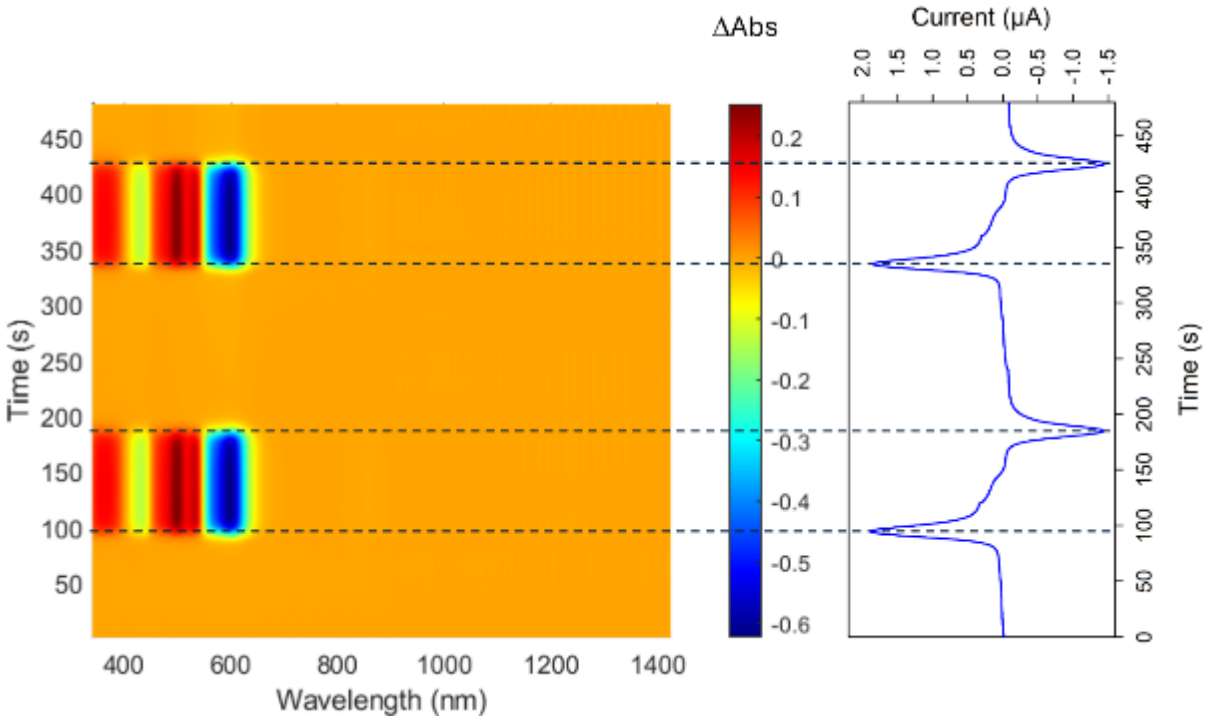

*Figure S29: Absorption variation recorded by real-time absorption spectroelectrochemistry of iminophosphorane-PDI **5** under thin-layer conditions in 1 mM CH_2Cl_2 with n-Bu_4NPF_6 (0.1 M in CH_2Cl_2), using Pt as the working electrode.*

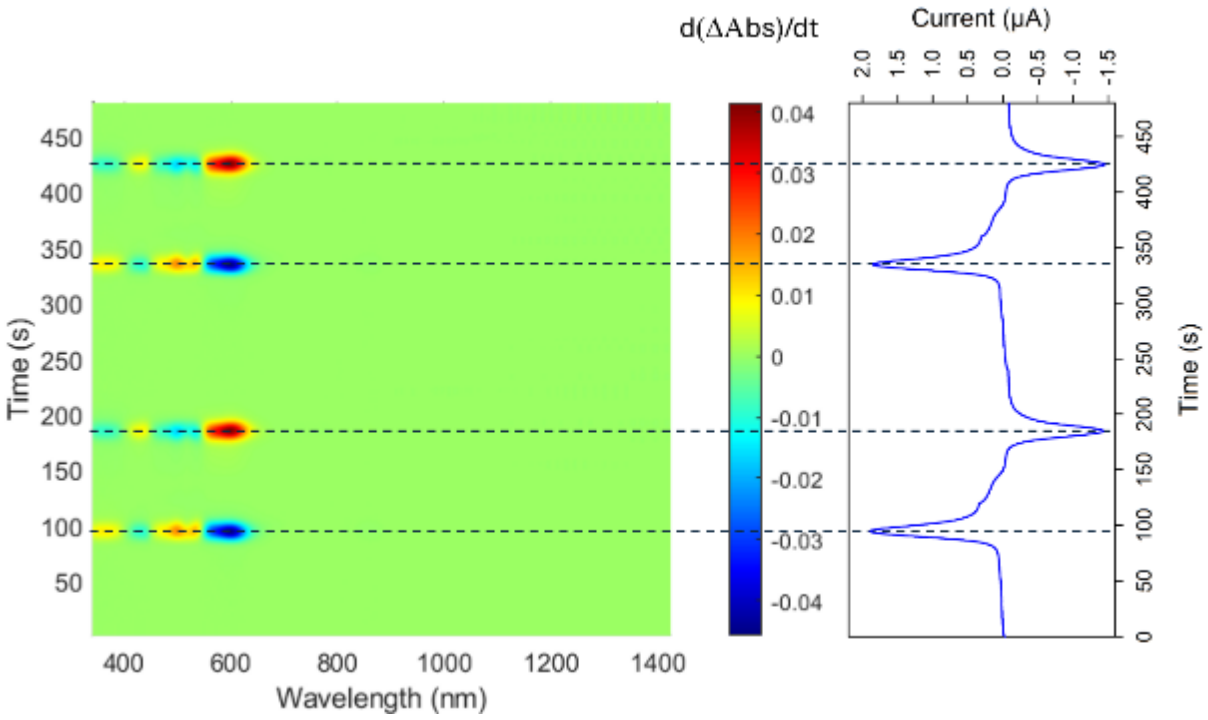

*Figure S30: Absorption variation derivative recorded by real-time absorption spectroelectrochemistry of iminophosphorane-PDI **5** under thin-layer conditions in 1 mM CH_2Cl_2 with n-Bu_4NPF_6 (0.1 M in CH_2Cl_2), using Pt as the working electrode.*

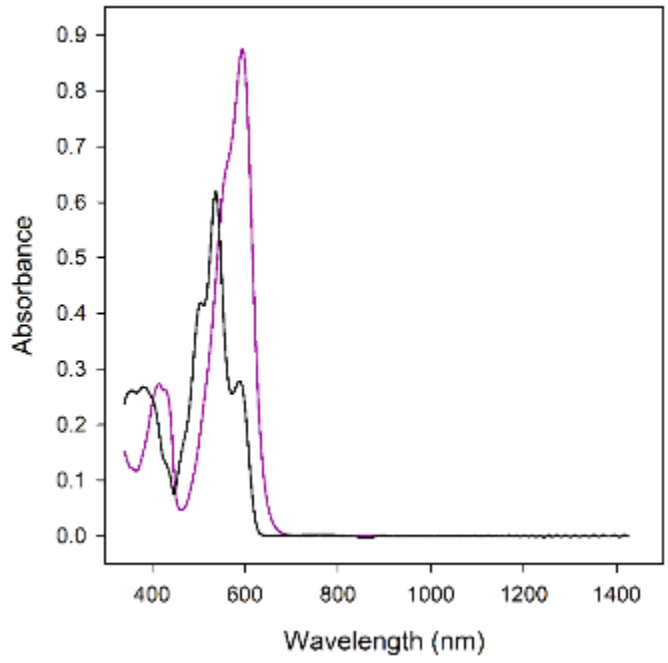

*Figure S31: Absorption spectra of iminophosphorane-PDI **5** in neutral state (purple) and in oxidized state (black).*

5. Thermogravimetric Analysis

The samples (weight 4.0 mg) were heated with a rate of 10 °C/min under N2. The thermal decomposition temperature (Td) was measured at 5% mass loss of the samples.

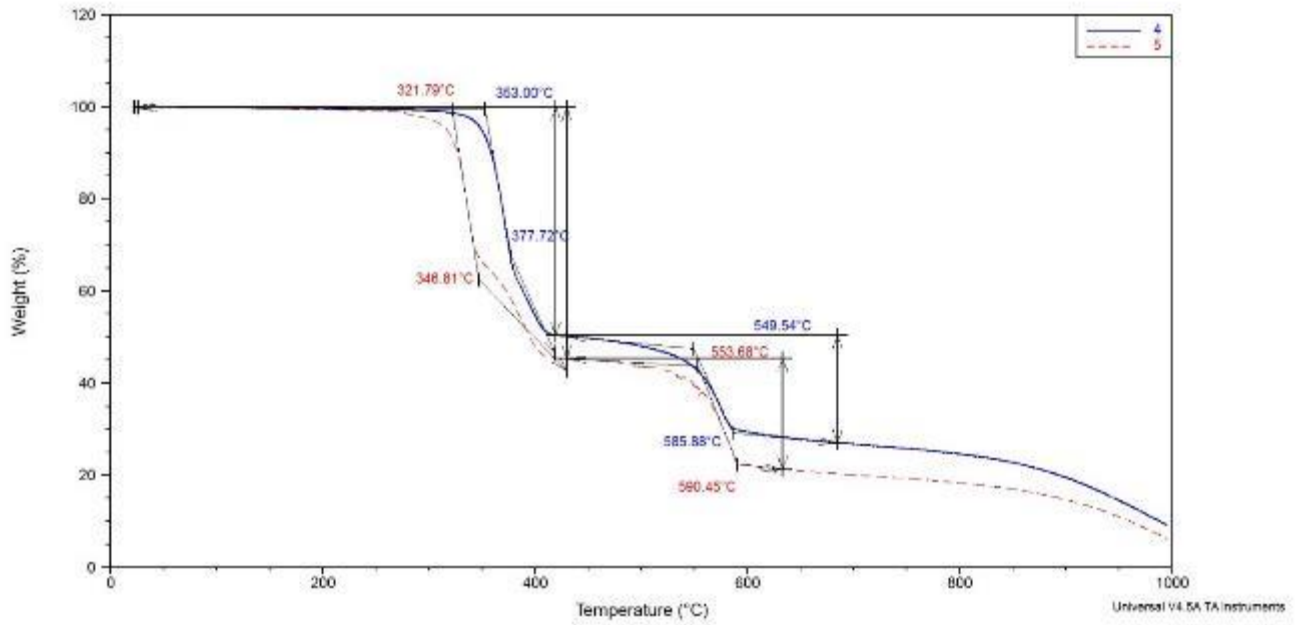

*Figure S32: Thermogravimetric spectra of compounds **4** (blue) and **5** (red).*

6. pH sensing experiments

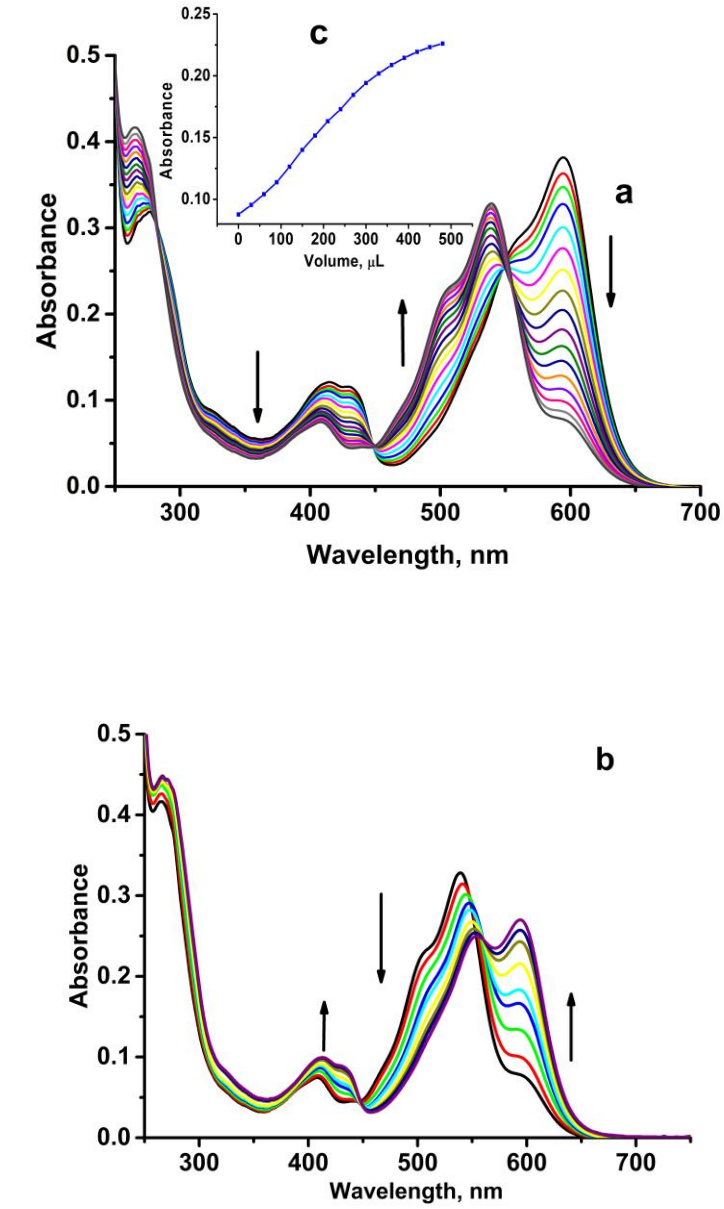

*Figure S33: Iminophosphorane PDI **5** at 10^{-5} M in CH_2Cl_2 during spectrophotometric titration by: **a)** a solution of H^+PPh_3,BF_4^- at 10^{-4} M in CH_2Cl_2; each addition of 30 μL corresponds to 0.12 equivalent of acid H^+PPh_3,BF_4^-; **b)** and subsequent addition of a solution of imidazole at 10^{-3} M in CH_2Cl_2; **c)** evolution of the absorption at 526 nm during the titration by a solution of H^+PPh_3,BF_4^- at 10^{-4} M in CH_2Cl_2.*

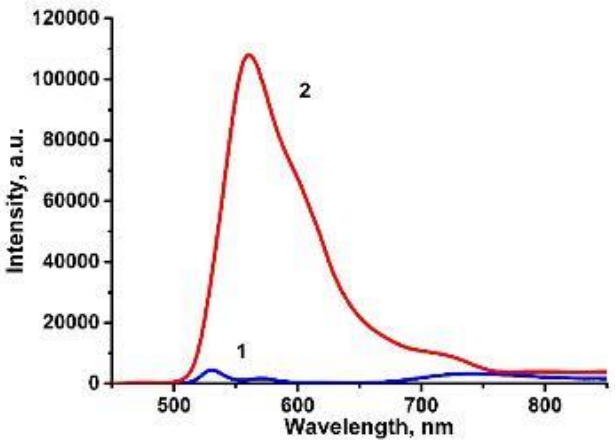

*Figure S34: Fluorescence emission spectrum of compound **4** ($C = 10^{-5}$ M, λ_{exc} = 420 nm) before -1 and after -2 spectrophotometric titration by solution of H^+PPh_3,BF_4^- in CH_2Cl_2 at 298K.*

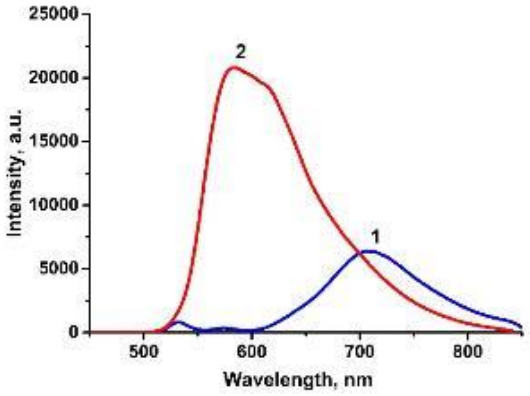

*Figure S35: Fluorescence emission spectrum of compound **5** ($C = 10^{-5}$ M, λ_{exc} = 420 nm) before -**1** and after -**2** spectrophotometric titration by solution of H^+PPh_3,BF_4^- in CH_2Cl_2 at 298K.*

*Figure S36: Photographic images of compound **4** before (A) and after addition of different acids:*

***A** : Compound **4** at 10^{-5}M in CH_2Cl_2 as reference; **B** : after addition of 5 µL HCl conc.; **C** : after addition of 5 µL H_2SO_4 conc.; **D** : after addition of 5 µL TFA; **E :** after addition of 100 µL glacial AcOH at t = 0 and **F** : after 16h.*

*Figure S37: Photographic images of compound **4** and **5** before (A and C) and after addition of HCl 0.1M (B and D)*

***A** : Compound **4** at 10^{-5}M in CH_2Cl_2 as reference; **B** : after addition of 5 µL HCl 0.1 M solution in CH_2Cl_2*
***C** : Compound **5** at 10^{-5}M in CH_2Cl_2 as reference; **D** : after addition of 5 µL HCl 0.1 M solution in CH_2Cl_2*

*Figure S38: Photographic images of compound **4** (A) in the presence of HCl (B) and after addition of imidazole (C)*

***A** : Compound **4** at 10^{-5}M in CH_2Cl_2 as reference ; **B** : after addition of 5 µL HCl 0.1 M solution in CH_2Cl_2 ; **C** : after sequential addition of 100 µL Imidazole 10^{-3}M in CH_2Cl_2.*

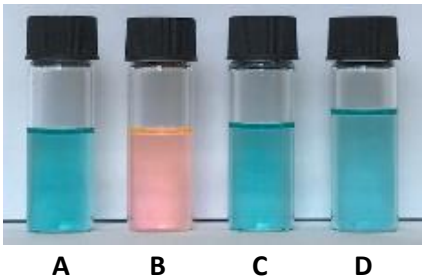

*Figure S39: Photographic images of compound **4** (A) and in the presence of H^+PPh_3,BF_4^- (B) and demonstration of the reversiblity after addition of imidazole (C), shown after 10 cycles of protonation-deprotonation (D)*

***A** : Compound **4** at 10^{-5}M in CH_2Cl_2 as reference ; **B** : after addition of 50 µL H^+PPh_3,BF_4^- 10^{-3}M in CH_2Cl_2 ; **C** : after addition of 50 µL H^+PPh_3,BF_4^- 10^{-3}M in CH_2Cl_2 then 50 µL Imidazole 10^{-3}M in CH_2Cl_2 ; **D** : after 10 cycles of subsequent addition of 50 µL H^+PPh_3,BF_4^- 10^{-3}M in CH_2Cl_2 then 50 µL Imidazole 10^{-3}M in CH_2Cl_2*

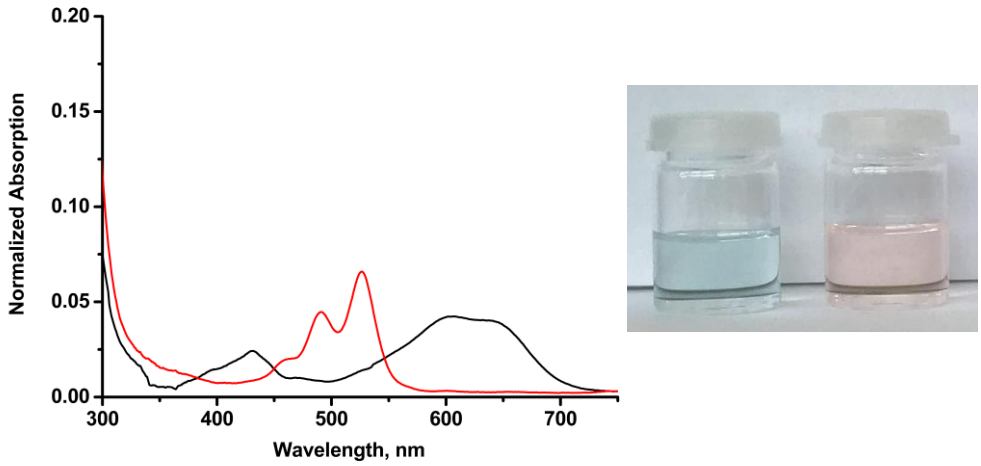

*Figure S40: UV-Visible spectra of iminophosphorane-PDI **4** at 10^{-6} M in CH_2Cl_2 (black) and after addition of a solution of H^+PPh_3,BF_4^- 10^{-3} M in CH_2Cl_2 (red). Photographic images of compound **4** (4 mL) (left) and after addition of a solution H^+PPh_3,BF_4^- 10^{-3} M (100 µL) (right).*

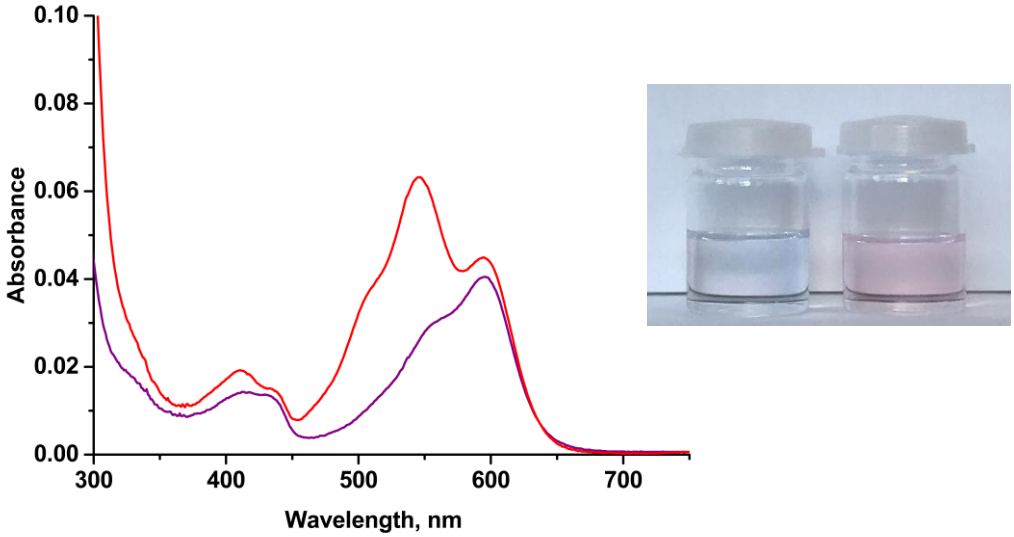

*Figure S41: UV-Visible spectra of iminophosphorane-PDI **5** at 10^{-6} M in CH_2Cl_2 (violet) and after addition of a solution of H^+PPh_3,BF_4^- 10^{-3} M in CH_2Cl_2 (red). Photographic images of compound **5** (4 mL) (left) and after addition of a solution H^+PPh_3,BF_4^- 10^{-3} M (100 µL) (right).*

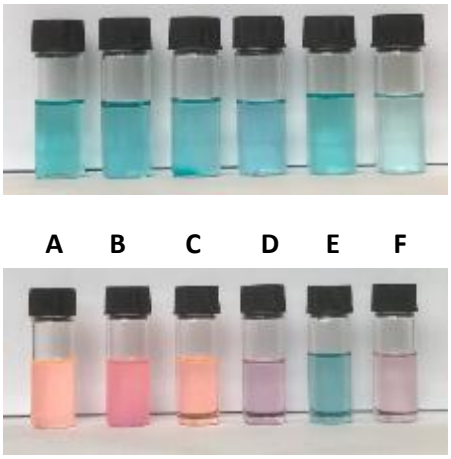

*Figure S42: Photographic images of compound **4** (A) in different solvents (top) and after addition of H^+PPh_3,BF_4^- (bottom)*

*Top : Compound **4** at 10^{-5}M in **A** : CH_2Cl_2, **B** : Toluene, **C** : EtOAc ; **D** : Et_2O ; **E** : DMF ; **F** : EtOH*
*Bottom : Compound **4** after addition of $HBF_4.Et_2O$ (5 µL)*
It is noted that no change of colour was occurring in DMF suggesting a preferential protonation of the solvent

*Figure S43: Photographic images of compound **4** at 10^{-4} M in CH_2Cl_2 solution (A) and after addition of 10 µL $HBF_4.Et_2O$ (B). Under emission lamp at 420 nm for compound **4** (C) and for protonated form (D).*

*Figure S44: Photographic images of compound **5** at 10^{-4} M in CH_2Cl_2 solution (A) and after addition of 10 µL $HBF_4.Et_2O$ (B). Under emission lamp at 420 nm for compound **5** (C) and for protonated form (D).*

*Figure S45: Iminophosphorane PDI **4** (left) in thin film (blue colour) and after addition HCl vapors (pink colour). Iminophosphorane PDI **5** (right) in thin film (violet colour) and after addition HCl vapors (magenta colour).*